Multiphoton dissociation of sf6 by a molecular beam method — **Source link**

Peter A. Schulz, Aa. S. Sudbo, Edward R. Grant, Y. R. Shen ...+1 more authors

Related papers:

- Multiphoton Dissociation of Polyatomic Molecules

- The extent of energy randomization in the infrared multiphoton dissociation of sf6

- Molecular dissociation of SF6 by ultra-short CO2 laser pulses

- Simple bond rupture reactions in multiphoton dissociation of molecules

- Is Multiphoton Dissociation of Molecules a Statistical Thermal Process

Lawrence Berkeley National Laboratory

Title
MULTIPHOTON DISSOCIATION OF SF6 BY A MOLECULAR BEAM METHOD

Permalink
https://escholarship.org/uc/item/160730dm

Author
Schulz, P.A.

Publication Date
1979-09-01

Lawrence Berkeley Laboratory
UNIVERSITY OF CALIFORNIA

Materials & Molecular Research Division

MULTIPHOTON DISSOCIATION OF SF_6 BY A MOLECULAR BEAM METHOD

P. A. Schulz, Aa. S. Sudbø, E. R. Grant, Y. R. Shen and Y. T. Lee
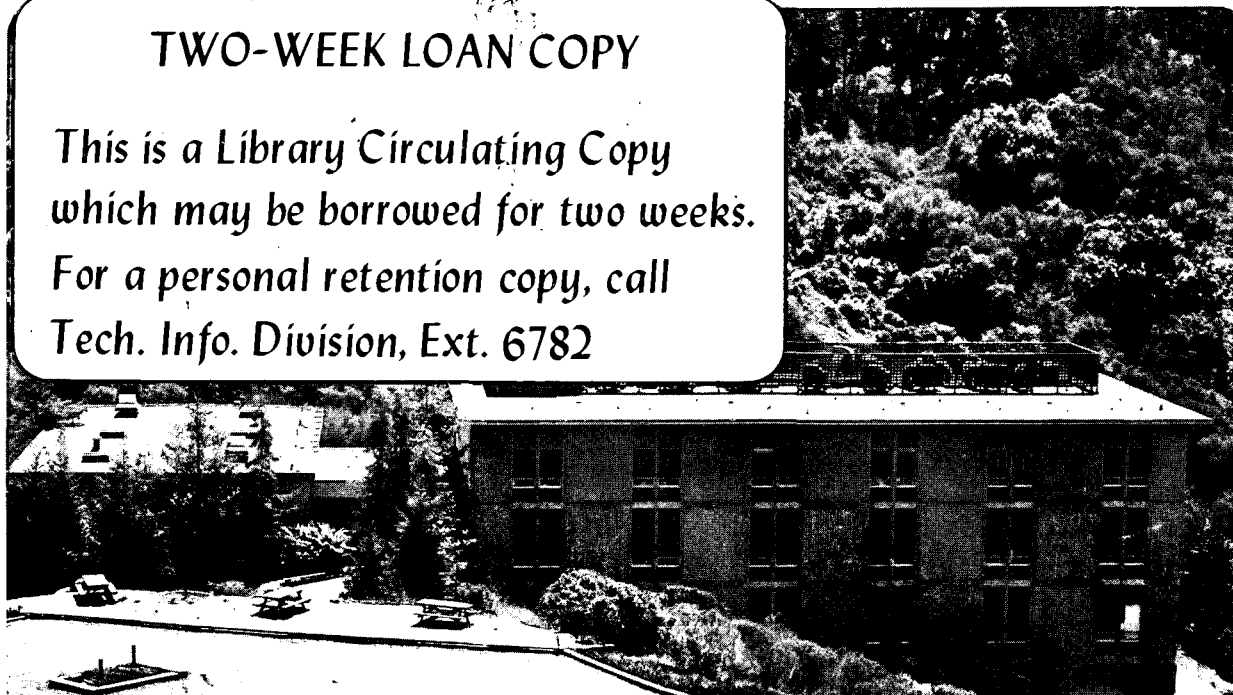
RECEIVED
LAWRENCE
BERKELEY LABORATORY

September 1979

OCT 15 1979

LIBRARY AND
DOCUM...

DISCLAIMER

MULTIPHOTON DISSOCIATION OF SF_6 BY A MOLECULAR BEAM METHOD

P. A. Schulz*, Aa. S. Sudbø*, E. R. Grant‡,

Y. R. Shen* and Y. T. Lee+

Materials and Molecular Research Division
Lawrence Berkeley Laboratory
University of California
Berkeley, California 94720

ABSTRACT

The dynamics of infrared multiphoton excitation and dissociation of SF_6 has been investigated under collision free conditions by a crossed laser-molecular beam method. In order to understand the excitation mechanism and to elucidate the requirements of laser intensity and energy fluence, a series of experiments have been carried out to measure the dissociation yield dependences on energy fluence, vibrational temperature of SF_6, the pulse duration of the CO_2 laser and the frequency in both one and two laser experiments. Translational energy distributions of the primary dissociation product, SF_5, measured by time of flight and angular distributions, and the dissociation lifetime of excited SF_6 as inferred from the observation of secondary dissociation of SF_5 into SF_4 and F during the laser pulse suggest that the dynamics of dissociation of excited molecules is dominated by complete energy randomization and rapid intramolecular energy transfer and can be

*Also associated with Department of Physics, Univ. of Calif., Berkeley.

+Also associated with Department of Chemistry, Univ. of Calif., Berkeley.

‡Present Address: Department of Chemistry, Cornell University, Ithaca, New York.

adequately described by RRKM theory. An improved phenomenological model including the initial intensity dependent excitation, a rate equation describing the absorption and stimulated emission of single photons, and the unimolecular dissociation of excited molecules is constructed based on available experimental results. Our studies show that although the energy fluence of the laser determines the dissociation yield of molecules in the quasi-continuum, the role played by the intensity of the laser in multiphoton dissociation is more significant than just that of overcoming the intensity dependent absorption in the lowest levels. Once molecules are excited beyond the dissociation energy, the average level of excitation of the dissociating molecules will be significantly influenced by the laser intensity for a given energy fluence when the rate of decomposition starts to compete with the rate of up-excitation.

INTRODUCTION

In recent years, a considerable amount of research activity has been directed toward understanding the phenomenon of infrared multi-photon dissociation (MPD) of molecules.[1-4] Sulfur hexafluoride has figured prominently in much of this research. It was among the first molecules to be dissociated by a high power CO_2 laser. Pressure dependence of isotopic selectivity in the MPD of SF_6[2-4] suggested that the dissociation took place under collisionless conditions. Later, molecular beam experiments confirmed this hypothesis.[5,6]

Early studies on the MPD products of SF_6 were interpreted to indicate (1) dissociation to SF_4 and F_2,[3,5] bypassing the lower energy SF_5 + F fragmentation channel and (2) absorption of 80 to 90 photons before dissociation.[7] These results led to the theoretical construction of coherent, mode-specific models for vibrational excitation in intense laser fields. More recent experiments, including the ones reported here, have shown that the primary dissociation occurs via a S-F bond scission.[6,8-11] The translational energy distributions of the fragments seem to imply that the excitation energy is completely randomized before decomposition. Experimental limits placed on the lifetime for decomposition[11] and a recent measurement of the total number of photons absorbed before decomposition[12] are in agreement with the assumption of randomization of the vibrational energy within the molecule. Lyman and Rockwood[13] and Black et al.[14] found that the energy fluence, not the intensity, determines the dissociation yield. Simple, incoherent sequential excitation models have been found to fit much of the data.[15,16]

The well-accepted, qualitative model for MPD of SF_6 involves, first, a near-resonant absorption of 3-6 infrared photons in a single vibrational ladder. Anharmonicity causes a mismatch between the vibrational spacing and the laser frequency which is nearly compensated by mechanisms such as allowed rotational transitions. At higher energy the density of states becomes large, and intermode coupling is strong so that the energy states of the molecules form a quasi-continuum. Further excitation of the molecules through this quasi-continuum occurs via resonant stepwise single-photon absorption. Eventually, the molecules are excited beyond the dissociation energy and dissociate. Because the energy is completely randomized in the SF_6 molecule, the dissociation can be described by a standard statistical theory of unimolecular reactions such as the RRKM theory. Statistical theory predicts that dissociation rates increase rapidly with increasing excess energy (i.e., excitation energy minus the dissociation energy) in the molecule and soon dissociation of the molecules starts to compete with up-excitation of the molecules by the laser. Hence, when the energy fluence of the laser is sufficiently high, most of the molecules will dissociate from excitation levels where the dissociation rate is roughly equal to the upexcitation rate.

MPD experiments performed on SF_6 in a molecular beam apparatus have provided a large body of information useful in elucidating the details of the MPD of SF_6. Measurements of the angular and time-of-flight distributions of the products, which have been reported previously,[6,10,11] probe the dynamics of dissociation. In order to provide a more complete picture of MPD of SF_6, we have extended our studies to investigate the dependence of the MPD yield on the amount of internal excitation in SF_6.

The absorption of photons by SF_6 depends upon the frequency and power of the infrared radiation as has been observed in many previous experiments (see Ref. 1). By performing the experiments in a molecular beam apparatus, we have been able to obtain information that is not available in a gas cell experiment. In particular, the vibrational temperature of SF_6 in a molecular beam has been varied while keeping the rotational temperature relatively low in order to study the absorption under different initial conditions. These new results in conjunction with earlier results enable us to produce a more realistic model to describe the MPD of SF_6.

EXPERIMENTAL

Our experiments were carried out by a molecular beam method in which a collimated molecular beam with a narrow well-defined velocity distribution was crossed by a pulsed CO_2 laser beam. The fragments resulting from MPD of the beam were detected as a function of angle by a rotatable quadrupole mass spectrometer with an electron bombardment ionizer. The direct identification of primary dissociation fragments and the measurements of their velocity and angular distributions under various experimental conditions were the basis for deriving information on the dynamics of MPD of SF_6.

The molecular beam of SF_6 was formed by expansion of neat SF_6 typically from 150 torr through a 0.1 mm diameter quartz nozzle. The average velocity of the SF_6 beam was 3.25×10^4 cm/sec and the velocity spread could be characterized by a speed to width ratio of $v/\Delta v = 4$ where Δv is the FWHM velocity spread. Three stages of differential pumping were used to obtain a well-defined beam of 2 mm diameter and $\sim 1^O$ FWHM angular spread. The SF_6 beam density at the point where it crossed with the CO_2 laser was estimated to be 10^{-5} torr, compared with a total background pressure of 5×10^{-7} torr.

The internal translational temperature of SF_6 in the molecular beam was measured from the FWHM velocity spread of the beam to be $T_r \sim 20K$. In the expansion, the rotational (R) and vibrational (V) temperatures of SF_6 may be different from the internal translational temperature of the beam. Lambert et al.[17] measured that 1005 collisions are required to cool SF_6 by $V \rightarrow T$ energy transfer. This was approximately 25 times the number of collisions that occured in the expansion.

Therefore the internal vibrational temperature of SF_6 in the beam was very close to the temperature of SF_6 prior to the expansion. The rotational temperature of SF_6 in the beam could be measured from the average translational energy of the beam that depends on the initial pressure. In the isenthalpic expansion to form the molecular beam, the translational energy of the beam should be:

$$E_{tr} = kT + \frac{3}{2} k(T-T_t) + \frac{3}{2} k(T-T_r)$$

The initial temperature prior to expansion, T, was 300K. Therefore, the rotational temperature, T_r, was approximately 150K after the expansion. By cooling and heating the nozzle, the influence of vibrational temperature on MPD of SF_6 was studied. Cooling and heating the nozzle may affect the rotational temperature of SF_6 in the beam to some extent, but the rotational temperature was lower than the vibrational temperature and thus was subject to smaller temperature changes. Nozzle temperatures of up to 500 K were achieved by a simple electrical heater wound around the nozzle. A liquid nitrogen cooled arm thermally connected to the nozzle was used to cool the SF_6 down to 210 K prior to expansion.

The interaction region was defined by the intersection of the molecular beam and the partially focused output of a grating tuned CO_2 laser. The CO_2 laser, a Tachisto 215G, delivered a 2 Joule pulse in a 60 ns FWHM spike followed by a 600 ns tail. The tail contained about 40% of the total energy. For certain experiments the temporal characteristics of the laser pulse were modified. A shorter laser pulse duration was obtained using a discharge shutter consisting of two 13 cm focal length ZnSe lenses placed 26 cm apart. These produced

air breakdown on the leading edge of the pulse and provided a truncated

output of about 15 ns FWHM with no tail. The laser pulse was then focused

into the scattering chamber by a 25 cm focal length ZnSe lens. The laser

pulse energy entering the interaction region was adjusted using external

attenuators. The cross sectional area of the laser beam in the interac-

tion region could be controlled by adjusting the position of the lens

to vary the distance from the focal point to the interaction region.

The energy fluence was then determined by a measurement of the laser

energy and the area of the laser beam in the interaction region. The

energy fluence fluctuation was less than 50% including spatial and pulse

to pulse variations. A slanted pyrex dish was used after the interaction

region in the vacuum chamber to absorb the 10μ radiation to prevent

photodesorption of adsorbed molecules from the surface of the stainless

steel chamber. Elastic scattering of SF_6 from the desorbed particles

was a source of contamination in Ref. 6.

In order to investigate the absorption process in more detail, MPD

of SF_6 was also carried out with two Tachisto 215G CO_2 lasers operating

at two different frequencies. One laser excited SF_6 up the discrete

vibrational ladder to the quasi-contimuum and the other provided suffi-

cient energy fluence to decompose the SF_6 molecules in the quasi-continuum.

The second laser was tuned to a frequency which was not absorbed by cold

SF_6. In this way the quasi-continuum absorption could be studied

separately from the initial 3-6 photon absorption.

The fragments from the interaction region were monitored by the

rotatable detector which has been described previously.[18] Briefly,

a set of 3 mm x 3 mm collimating slits on the walls of the triply

differentially pumped detector insured an angular resolution of 1^O (0.5 millisteradian solid angle). The innermost region at a pressure of less than 10^{-10} torr contained a 200 eV coaxial electron bombardment ionizer of the Brinks type. The ionized molecular fragments were focused and analyzed by a quadrupole mass filter. The ions were counted using a Daly type scintillation ion counter. A typical background count rate for the SF_3^+ ion with the SF_6 molecular beam on was 10^5 counts/sec at 5° away from the beam.

The electronics setup for data collection is shown schematically in Fig. 1. The laser(s) was fired at a rate of 0.7 Hz by a pulse generator. For the measurement of angular distributions the pulse generator was also used to trigger two gates. One gate enabled the first channel of a dual channel scaler after an initial delay that allowed the fragments to arrive at the detector. The scaler accumulated signal from the detector's ion counter for a gate width corresponding to the width of the flight time distribution (around 0.8 ms). Then after a second delay of 10 ms the other channel of the scaler was enabled by the second gate to count background for the same gate width time.

Velocity distributions of the fragments were measured by the time-of-flight method using a multichannel scaler (either a Hewlett-Packard 5422B Digital Processor or a 256-channel scaler interfaced with a Nova 1220 minicomputer). The trigger pulse for the laser was also used to start the time sweep for the multichannel scaler. The delay between the trigger for the laser and the laser pulse was measured by a photon drag detector to be less than 1 μs. This delay was

unimportant because the fastest flight time of sulfur containing fragments was more than 200 µs and the dwell time per channel was typically 10 µs. The time-of-flight spectrum was taken in 250 channels, which was long enough to collect the signal and to determine the baseline of background accurately.

RESULTS AND ANALYSIS

The first objective of this series of experiments is to determine the MPD products of SF_6. Some of these results have been reported previously[11] but are included here for completeness. SF_3^+ and SF_2^+ are the major ion fragments observed in the ionizer from the neutral molecular fragments of SF_6 under MPD. Time-of-flight spectra and angular distributions of SF_3^+ and SF_2^+ are identical, with a signal ratio $SF_3^+:SF_2^+$ of $4.5 \pm 0.5:1$ when using a 5 J/cm^2 CO_2 laser pulse tuned to 944 cm^{-1} (see Fig. 2). The $SF_3^+:SF_2^+$ ion fragmentation ratio from SF_4 is measured to be 2.2:1 using 200 eV electrons. We expect that the $SF_3^+:SF_2^+$ ratio produced in the ionizer for SF_5 should be greater than the ratio observed for SF_4. The observed ratio of $SF_3^+:SF_2^+$ and the identical angular and velocity distributions of SF_3^+ and SF_2^+ are therefore indicative of SF_5, not SF_4, as the major product from MPD of SF_6. The possibility that the signal might arise from SF_6 entering the detector can also be ruled out since the SF_5^+ and SF_4^+ signals expected from the electron impact fragmentation of SF_6 were not observed. Thus, we conclude that in our experiment, at moderately low laser fluence (< 8 J/cm^2), MPD of SF_6 yields predominantly the products SF_5 and F.

When the energy fluence of the CO_2 laser pulse at 944 cm^{-1} is increased to 15 J/cm^2, the angular distributions of the SF_3^+ and SF_2^+ ion fragments (see Fig. 2) differ from each other, indicating the presence of additional neutral fragments from MPD. The $SF_3^+:SF_2^+$ signal ratio changes from about 4:1 at 5^0 to 2.5:1 at 30^0 from the SF_6 beam. The $SF_3^+:SF_2^+$ ratio at large angles is indicative of the appearance of a secondary product, namely, SF_4. One might think that

the change in the $SF_3^+:SF_2^+$ ratio is caused by an increase in internal excitation of the SF_5 fragment from MPD of SF_6. At increased laser power, SF_6 is excited to higher energy before dissociating, producing SF_5 which also has higher internal excitation. If this is true, then the $SF_3^+:SF_2^+$ ratio would change continuously with the energy fluence, but be nearly independent of the angle. However, the observations in this experiment are that the $SF_3^+:SF_2^+$ ratio changes dramatically with angle, and also rapidly with energy fluence, from 4.5:1 at 5 J/cm^2 to 2:1 at 20 J/cm^2. The hypothesis that SF_4 and F_2 may be the products of SF_6 MPD competing with dissociation into SF_5 and F is also inconsistent with this experiment. First, no F_2^+ is observed in the mass spectrometer. Second, dissociation of SF_6 into SF_4 and F_2 is likely to have an energy barrier in the exit channel that should lead to a very broad angular distribution of the fragments, as has been observed in other three center elimination reactions.[19] Such an angular distribution is not observed. Therefore, we conclude that at high energy fluence SF_5, formed by MPD of SF_6, absorbs 944 cm^{-1} laser radiation and dissociates into SF_4 and F.

Some of our most significant findings concerning the dynamics of MPD are contained in our angular and velocity distributions. After changing the laser polarization, no change is observed in the angular or time-of-flight distributions. This indicates that the velocity distribution of fragments in the center of mass frame is isotropic. The transformation of an isotropic product center of mass translational energy distribution to laboratory angular and velocity distributions for multiphoton dissociation has been discussed in detail elsewhere.[19]

Figure 3 shows the theoretical and experimental velocity distributions of SF_5 detected as SF_3^+ produced by a laser energy fluence of 5 J/cm^2. The theoretical curves were calculated from the translational energy distributions shown in Fig. 4. The energy distributions were derived from the RRKM statistical theory of unimolecular dissociation. The RRKM theory only predicts the dissociation rate constant and the translational energy distribution of the fragments in the critical configuration. However, for loose complexes[19,20] the absence of barriers in the exit channel makes the translational energy distribution of the fragments in the critical configuration essentially the same as the final translational energy distribution of the fragments. The theory assumes that a molecule excited above the dissociation level randomly samples the available vibrational phase space in the process of decomposition. The agreement between theory and experiment on the translational energy distributions strongly supports this assumption. Many accounts have already been given of the RRKM theory and the calculation of dissociation rate constants[11,16,20,21] and will not be repeated here. However it should be pointed out that a discrepancy which appeared in the literature on the dissociation rate constants for SF_6 has now been resolved. The previous results of this group[11] gave significantly higher rate constants than Lyman's calculations[16] because we used a dissociation energy of D = 77 kcal/mole rather than the dissociation energy of D = 93 kcal/mole.[16] The results of our RRKM calculation using D = 93 kcal/mole agree with the results reported in Ref. 16 (see Appendix).

The results we obtain from the study of angular and velocity distribution of fragments are summarized as follows: 1) the translational energy distribution peaks at less than 0.2 kcal/mole. This means that no appreciable exit potential energy barrier exists along the reaction coordinate. It also implies no significant centrifugal barrier; thus, SF_6 must have acquired negligible average angular momentum in the multiphoton excitation process. 2) The fit of the RRKM translational energy distributions to the experimental ones indicates that at an energy fluence of $5J/cm^2$, the SF_6 molecules achieve excess energies of 16 to 27 kcal/mole before dissociating. 3) Of the 16 to 27 kcal/mole excess energy, only an average of 2.5 kcal/mole appears as translational energy of the fragments. 4) Because the rotational and translational energies are small, most of the excess energy is left as internal excitation in SF_5 (13 to 24 kcal/mole). Consequently the SF_5 fragment is already excited to the quasi-continuum. It can readily absorb more radiation, even if the laser frequency is significantly different from the fundamental absorption frequency of ground state SF_5. With sufficient energy fluence, SF_5 is excited beyond its own dissociation energy, and dissociates into SF_4 + F.

An attempt was made to find the translational energy of SF_4 and F produced in the secondary MPD of SF_5. The angular distribution is obtained over a limited range of angles ($>15^o$) where the $SF_3^+:SF_2^+$ ratio is measured to be about 2.5:1 so that the MPD fragment is mainly SF_4. At angles less than 15° the $SF_3^+:SF_2^+$ ratio is significantly larger than 2.5:1, even with a laser energy fluence of 50 J/cm^2. At these high energy fluences, the laser does not uniformly illuminate the interaction

region so that a considerable amount of SF_6, subject to energy fluences below 10 J/cm^2, does not undergo a two step dissociation to form SF_4. With the limited angular range over which the SF_4 fragment could be measured, the average translational energy released in the fragmentation $SF_5 \rightarrow SF_4 + F$ could be determined only approximately. We find that the average energy released is between 0.5 and 1.5 kcal/mole.

Figure 5 shows the angular distribution of SF_3^+ obtained with 5 J/cm^2 and 3 J/cm^2 laser pulses and a 2.5 J/cm^2 pulse shortened by a plasma shutter. The RRKM theoretical calculations for the angular distributions at various excess energies are shown for comparison. The fits to the angular distributions obtained with 5 and 3 J/cm^2 pulses have average excess energies of ~22 kcal/mole (8 CO_2 laser photons) and ~13 kcal/mole (5 CO_2 laser photons), respectively. The 2.5 J/cm^2 shuttered pulse seems to have excess energy less than 8 kcal/mole (< 3 CO_2 laser photons). The corresponding dissociation lifetimes predicted by the RRKM theory are 20 ns, 1 μs, and 20 μs, respectively. It should be noted that using the 2.5 J/cm^2 pulse, the angular distribution appears to deviate from the RRKM prediction. This is due to our experimental arrangement. In our apparatus (although the entire interaction region is monitored by the detector at all angles) the segment of the molecular beam monitored by the detector varies with the angular position of the detector. At 5 degrees, a 15 mm long segment is monitored, but at 25 degrees, only a 3 mm segment is monitored. The corresponding transit times for SF_6 to move through the detectable segment are 50 μs and 10 μs respectively. Therefore, any SF_6 molecules that absorb less than four excess photons have life times longer (more

than 10 μs) than the transit time through the interaction region and can be seen by the detector only at small angles. Consequently, the observed angular distribution of SF_5 is weighted toward small angles and appears more sharply peaked than the RRKM prediction.

Figure 6 shows the frequency dependence of SF_6 MPD for vibrational temperatures between 210K and 450K. The energy fluence used is 5 J/cm^2 with a maximum power density over 100 MW/cm^2. The MPD yield spectrum is effectively broadened from 8.5 cm^{-1} at 210K to 18 cm^{-1} at 380K to >20 cm^{-1} at 450K. The MPD yield spectrum at 295K has a peak at 943 cm^{-1} and a FWHM spread of ~14 cm^{-1}. This result qualitatively agrees with that reported by Ambartzumian et al.[3] whose spectrum has a peak at 941 cm^{-1} and a spread of ~18 cm^{-1}. When the vibrational temperature is either raised or lowered, the yield remains approximately the same at frequencies higher than 943 cm^{-1}. At lower frequencies, raising the vibrational temperature dramatically increases the MPD yield. These results suggest that the dissociation yield at higher laser frequencies (>943 cm^{-1}) is limited only by excitation through the quasi-continuum while the dissociation yield at lower frequencies is limited by excitation over the discrete levels. We show in Table 1 the vibrational population distributions at the four temperatures used in this experiment. At 210K 63% of the molecules are in the ground vibrational state. Therefore, the frequency dependence of MPD at 210K probably reflects quite closely the frequency dependence of MPD of ground vibrational state SF_6. The presence of vibrationally hot molecules at room temperature affects the MPD yield spectrum by increasing the amount of dissociation at low frequency. Cooling of SF_6 thus results in the disappearance of MPD at low frequency.

Many gas cell experiments have been performed to measure the SF_6 MPD yield as a function of energy fluence at several different CO_2 laser frequencies. Kwok and Yablonovitch[22] have recently shown that even for SF_6 barely excited to the quasi-continuum, the collisional relaxation time is τ_{coll} = 13 ns-torr/p where p is the SF_6 gas pressure. In a gas cell experiment holes burned in the rotational population distribution by the laser may be filled by collisional relaxation even at moderately low pressures. Then, both the energy fluence and frequency dependences of the MPD yield are affected. Therefore it is important to measure these dependences in a collision-free molecular beam experiment.

Figure 7 shows the energy fluence dependence of MPD of SF_6 at three different laser frequencies. Since the experiments are performed with the same laser pulse duration, it is important to note that the power of the laser is also varied proportional to energy fluence. At 935 cm^{-1}, MPD is observed at energy fluences as low as 1-2 J/cm^2 and the yield increases slowly with increasing energy fluence. At 944 cm^{-1} the SF_6 MPD threshold is observed at higher energy fluence but the dissociation yield increases very rapidly with increasing fluence. At 953 cm^{-1} SF_6 MPD is first observed at even higher fluence, but the yield increases slowly with fluence. Measurements at other frequencies between 935 and 953 cm^{-1} have also been made; the yield curves are intermediate between the ones shown. Figure 8 shows the energy fluence threshold for dissociation as a function of frequency obtained from plots similar to Figure 7. Our results agree with those of Gower and Billman[23] and disagree with those of Brunner and Proch[24], that is, the threshold at 935 cm^{-1} is four times lower than the

threshold at 952 cm^{-1}. The low energy fluence threshold at low frequency is caused by a larger quasi-continuum cross section at low frequency. However, the bottleneck prevents a lot of dissociation from occuring at low frequency. At high frequency (near the ν_3 resonance) the quasi-continuum cross section is small so the energy fluence threshold is large and the bottleneck is relatively unimportant.

In general the experimental results are affected by several important factors. We briefly describe these factors here and again in more detail in the discussion section.

(1) The hot band absorption becomes increasingly important at higher temperatures and at frequencies below 943 cm^{-1}. It lowers the laser intensity necessary to pump the molecules into the quasi-continuum.

(2) Low intensity laser radiation is only effective in exciting a small fraction of the rotational population into the quasi-continuum. Thus, the frequency dependence of MPD at low laser intensity should depend on the population distribution in the rotational states.

(3) With the laser pulse duration kept constant, increasing the energy fluence increases the intensity. The increased intensity results in more molecules pumped into the quasi-continuum.

(4) The absorption spectrum of molecules in the quasi-continuum shifts to lower frequency as the level of excitation increases. This has been shown by the experiments of Nowak and Lyman[25] and Bott.[26]

Two frequency experiments are designed to decouple the absorption in the region of the discrete vibrational ladder from that in the quasi-continuum. The first laser excites a certain fraction of the SF$_6$ molecules into the quasi-continuum where some further excitation

may occur, depending on the energy fluence in the pulse.[27] The second
laser then interacts with three different groups of SF_6 molecules:
(1) ground state molecules, (2) vibrationally excited molecules in the
low lying discrete levels, and (3) molecules in the quasi-continuum.
By being sure that the second laser alone does not cause dissociation
of SF_6, we can neglect the contribution of the ground state SF_6 to the
dissociation yield. If the second laser is at a frequency sufficiently
far above the molecular resonant frequency, the MPD of vibrationally
excited molecules in the discrete levels also becomes relatively
insignificant.

Figure 9 gives our results on the frequency dependence of the MPD
yield of SF_6 using two lasers, one fixed at 1060 cm^{-1} and the other
tuned through the ν_3 resonance of SF_6. It is seen that the dependence
of MPD on the frequency of the second laser is significantly narrower
and shifted to higher frequency than the one obtained with a single
laser. These results are in good agreement with those of Ambartzumian
et al.[28] The major reason for the change in the frequency dependence
is that the intensity of the tuned laser in the two laser experiment
is lower than that in the one laser experiment. The decreased intensity
reduces the range of initial states that are coupled to the quasi-
continuum by the laser and results in a smaller MPD frequency spread.

MODEL CALCULATIONS

Recently, a number of calculations have been performed on the infrared MPD of SF_6[15,16,29] using the rate equation model. Here we extend the model calculations by explicitly considering the intensity dependent excitation over the discrete levels into the quasi-continuum and the two step dissociation process: $SF_6 \rightarrow SF_5 + F \rightarrow SF_4 + 2F$. These model calculations are compared with the experimental results just described. The good agreement between the model and the experiments implies that the model calculation provides a quantitative description of MPD of SF_6.

The rate equation model proposed in reference 15 is based on the following assumptions:

(1) The MPD yield is determined by the multiple stepwise excitation in the quasi-continuum and is not limited by the excitation over discrete levels.

(2) Coherent optical effects, spontaneous emission, and collisions are neglected in the excitation process.

(3) All molecules at approximately the same energy have the same absorption cross section.

(4) The ratio of the stimulated emission cross section to the absorption cross section is given by the ratio of the density of states of SF_6 in the levels involved.

(5) The dissociation rate constant at a given energy above the dissociation energy is given by the statistical RRKM model.

(6) The SF_5 dissociation product absorbs an insignificant amount of energy from the infrared field and thus any secondary MPD is ignored.

Here we present the model calculation with assumptions 1 and 6 eliminated. Following assumptions (2)-(5) the rate equations for molecules in the quasi-continuum are:

$$\frac{dN_m}{dt} = \frac{I(t)}{h\nu} \left[\sigma_{m-1}N_{m-1} + \frac{g_m}{g_{m+1}} \sigma_m N_{m+1} - \left(\frac{g_{m-1}}{g_m} \sigma_{m-1} + \sigma_m \right) N_m \right] - k_m N_m \quad (1)$$

where N_m is the normalized population in level m at energy $mh\nu$, $I(t)$ is the laser intensity, g_m is the density of states of level m, σ_m is the absorption cross section from level m to level m + 1, and k_m is the dissociation rate constant from level m calculated using the RRKM model (see appendix). The use of the RRKM model was justified in the previous section.

It is easily seen from Eq. (1) that if the dissociation is insignificant ($k_m = 0$), the excitation rate is proportional to the laser intensity. Time integration of the rate equations gives a population distribution which is only a function of laser energy fluence. In fact, our calculations show that for a given laser energy fluence the dissociation does not strongly affect the shape of the population distribution below the dissociation levels even if a significant fraction of the SF_6 has dissociated. This makes energy fluence an important parameter in the model calculation.

The density of states, g_m, is calculated with the Whitten-Rabinovitch approximation.[20] Use of this approximation tacitly assumes that the SF_6 molecules in the quasi-continuum are randomly distributed in the available vibrational states. There is the question of whether the rotational degrees of freedom should be included in the calculation

of the density of states. The upper limit of this effect is investigated by calculating the density of states with the rovibrational Whitten-Rabinovitch approximation.[20] At the onset of the quasi-continuum the ratio of density of states changes by only 4% (i.e., $(g_4/g_3)_{v,r} = 1.04(g_4/g_3)_v$), while at the dissociation level it changes by only 1%. These changes cause at most a 1% difference in the population of any level in a typical model calculation. Thus, inclusion of rotational degrees of freedom in the calculation of the density of states is not important in this rate equation model.

The absorption cross section and its dependence on excitation energy are very difficult to estimate from any ab-initio calculation. In our calculation the absorption cross section is assumed to decrease exponentially with excitation and is determined by a fit to the experimental results as we shall describe later.

To include multiphoton excitation of the SF_5 dissociation product and the subsequent secondary dissociation into SF_4+F in the model calculation, there should be a similar set of rate equations for SF_5:

$$\frac{dN_j(SF_5)}{dt} = \frac{I(t)}{h\nu}\left[\sigma_{j-1}N_{j-1}(SF_5) + \frac{g_j\sigma_j}{g_{j+1}}N_{j+1}(SF_5)\right.$$

$$\left. - \left(\frac{g_{j-1}}{g_j}\sigma_{j-1} + \sigma_j\right)N_j(SF_5)\right]$$

$$- k_jN_j(SF_5) + k_mN_m(SF_6) \tag{2}$$

where $m = j + D/h\nu$ and D is the dissociation energy of SF_6. The term involving $N_m(SF_6)$, indicates generation of SF_5 through dissociation of SF_6. Because the translational energy of the fragments is only a small fraction of the excess energy beyond the dissociation energy,

we assume that all the excess energy in SF_6 appears as internal energy in SF_5. Thus, the rate of appearance of SF_5 in a given level equals the dissociation rate of SF_6 from the corresponding level. The density of states for SF_5 is obtained from the Whitten-Rabinovitch approximation and the SF_5 dissociation rate constants from an RRKM calculation (see appendix). The absorption cross section is found by a fit of the calculation to the experimental data on the MPD of SF_5. The inclusion of multiphoton excitation of the SF_5 dissociation product provides a more accurate description of MPD of SF_6.

A more realistic model calculation should also include the intensity dependent 3-6 photon excitation over the discrete levels of SF_6. The existence of an intensity dependent "bottleneck" in the excitation into the quasi-continuum was originally suggested by Ambartzumian et al.[3] and subsequently shown experimentally.[14,28] Detailed quantum mechanical models of the discrete levels have been developed [3,30] which include the rotational substructure in the vibrational levels. The time development of the excited SF_6 population in the discrete levels has been calculated using such models.[31.32] However, they are too complex for simple calculation. We use here a much simpler, phenomenological approach.

The major assumption in this approach is that the excitation of population into the quasi-continuum from different rotational vibrational states requires different laser intensities. The bottleneck is a consequence of the fact that not all the molecules are in a single rotational-vibrational state. To illustrate this, assume that the quasi-continuum begins at an energy of 3h and that a single three

photon process is effective in exciting the population into the quasi-continuum. If we neglect stimulated emission, then the excitation rate can be assumed to be proportional to I^3. The rate of depletion of population, $N_{0,J}$, in the Jth rotational level of the ground vibrational state is given by:

$$\frac{dN_{0,J}}{dt} = -a_J I^3 N_{0,J}$$

and the solution is:

$$N_{0,J} = N_{0,J}(0) \exp\left[-a_J \int_0^t I^3(t')dt'\right] \tag{3}$$

where a_J is a constant different for different rotational-vibrational states. The rate at which the population is excited into the quasi-continuum is then equal to $-d(\sum_J N_{0,J}(t))/dt$. This should be included in the rate equation for $m = 3$ in Eq. 1 as an additional source term, i.e.,

$$\frac{dN_3}{dt} = \frac{g_3}{g_4} \sigma_3 N_4 - \sigma_3 N_3 - \frac{d}{dt}\left(\sum_J N_{0,J}\right) \tag{4}$$

For a usual bell-shaped pulse, the function $N_{0,J}(t)$ is close to a step function and can be further approximated by:

$$N_{0,J}(t) = N_{0,J}(0) \qquad \text{if } I_{max}(t) \leqslant I_J$$
$$= 0 \qquad\qquad \text{if } I_{max}(t) > I_J$$

where $I_{max}(t)$ is the maximum laser intensity during the time period between $-\infty$ and t and I_J is a value characteristic of the excitation of the Jth rotational-vibrational state to the quasi-continuum. This

is a reasonable approximation; it also makes the model insensitive to the exact excitation mechanism over the discrete levels which is probably not a single three photon process.[30-32] It should also be noted that $N_{0,J}$ only depends on $I_{max}(t)$.

For each of the many rotational states there is a different intensity, I_J, required to excite the molecules over the discrete states into the quasi-continuum. The I_J's are spread over a wide range of intensities reflecting the fact that the detuning of the laser frequency from resonance may be dramatically different for different rotational states. We therefore assume that the I_J's are approximated by a continuous distribution. The resulting $\sum N_{0,J}(I_{max}(t))$, instead of being a sum of step functions, becomes a continuously differentiable function. This function should satisfy the condition that very little population is excited over the discrete states into the quasi-continuum when the peak laser intensity, $I_{max}(t)$, is small. If the peak laser intensity is large nearly all the population should be excited over the discrete states into the quasi-continuum. As shown in Fig. 10 the curve represented by the function:

$$\sum_J N_{0,J}(I_{max}(t)) = \frac{1}{\sqrt{\pi}} \int_{\gamma \ln(I_{max}(t)/I_0)}^{\infty} e^{-x^2} dx$$

has these properties, e.g., $\sum_J N_{0,J} \to 1$ when I_{max} is small and $\sum_J N_{0,J} \to 0$ when I_{max} is large. Here, I_0 is the median of the I_J's and γ is a parameter characterizing the spread of I_j's.

This model is used to calculate the MPD of SF_6. The algorithm is a simple time integration of Eq. 1, 2, 4, and 6 with the initial condition that all the population is initially in the lowest level. By varying the time step for integration around 10ps, it is ascertained that round off errors are negligible. The laser pulse profile, $I(t)$, used in these calculations is shown in Fig. 11 and is representative of the pulse envelope from a Tachisto 215G laser ignoring the mode locking spikes of the pulse. The mode locking spikes in the 60ns multimode pulse were considered in our calculation by assuming that the mode locking doubles the peak intensity achieved by a single mode pulse. The limited time resolution of the detector and oscilloscope prevented us from measuring the actual peak intensity.

With the quasi-continuum absorption cross section assumed to have the form $\sigma_m = \sigma_0 e^{-\beta m}$, there are four independent parameters to be determined: γ and I_0 for excitation up the discrete vibrational ladder and σ_0 and β for excitation through the quasi-continuum. The parameters are chosen to fit the experimental results of Black et al.[12] on the average number of photons absorbed per molecule, $<n>$, versus energy fluence at 944 cm^{-1} using three different laser pulses: 0.6ns and 60ns single mode and 60ns multimode. We find that our calculation closely reproduces the experimental curves of Black et al.[12] with $\gamma = .5$, $I_0 = 20$ MW/cm^2, $\sigma_0 = 8.10^{-19}$ cm^2, and $\beta = .042$. This is shown in Fig. 12. The fit to the 0.6 ns pulse is insensitive to the parameters γ and I_0 in the calculation because the maximum laser intensity is much larger than I_0. So, the 0.6 ns pulse result is used to find σ_0 and β and the 60ns single mode pulse result is used to find γ and I_0.

The 60ns multimode pulse result agrees qualitatively with the model calculation, but seems to indicate that the intensity is more than twice the intensity of the single mode pulse, which is the assumption in the model calculation. That the multimode pulse achieves more than double the intensity of a single mode pulse has been observed by other groups using faster detectors and oscilloscopes.

The results obtained in our molecular beam apparatus are the only data on the multiphoton dissociation of SF_5. Therefore, we assume, from lack of data to the contrary, that the discrete vibrational states of SF_5 can be neglected because the SF_5 has enough vibrational energy to be in its quasi-continuum and that its quasi-continuum cross section is independent of the SF_5 energy (i.e., $\beta = 0$). The onset of secondary MPD of SF_5 observed experimentally agrees with the results of the model calculation using $\sigma_0 = 10^{-19}$ cm^2.

Figure 13 shows our model calculation for the dissociation yield versus energy fluence using a 60ns multimode laser pulse. The yield is nearly linear in energy fluence from 3 to 7 J/cm^2 in excellent agreement with the linear dependence experimentally observed at 944 cm^{-1} (see Fig. 7). At higher fluence, the SF_5 product disappears because it dissociates into SF_4 + F. The SF_4 yield grows quickly with energy fluence until there is 100% yield.

Grant et al.[15] showed that the population distribution in the quasi-continuum predicted by a model with no bottleneck is significantly narrower than a thermal distribution. The conclusion is also valid for this model calculation when the intensity dependence of excitation over the discrete levels is included. The model calculation with a

0.5 J/cm^2, 60ns FWHM laser pulse predicts that the population in the quasi-continuum is narrower than thermal even though only 20% of the molecules have been excited over the discrete states into the quasi-continuum. The population distribution is narrower than thermal whenever the cross section decreases with increasing excitation because the excitation rate for those molecules in the low energy tail of the distribution is large and the excitation rate in the high energy tail is small. Fig. 14 shows a comparison of the population distribution for a .5J/cm^2, 60ns laser pulse and for a .5J/cm^2, 15ns FWHM plasma shuttered laser pulse from our model calculations. In both cases the predicted population distribution is narrower than thermal. Because the plasma shuttered pulse achieves a higher intensity, the model predicts that more population is coupled into the quasi-continuum. The shape of the population distributions shown in Fig. 14 are similar but differ slightly because the maximum intensity of the shuttered pulse occurs at the end of the pulse, so population is being excited into the quasi-continuum at the end of the pulse. Thus, the shuttered pulse is slightly broader and peaks at a slightly lower energy. As the energy fluence is increased above .5 J/cm^2 the slight effect of the laser pulse shape on the population distribution becomes undetectable. The shape of the SF$_6$ population distribution is almost completely determined by the energy fluence if the energy fluence is greater than .5J/cm^2 and the laser pulse duration is less than 100ns. Because the quasi-continuum cross section decreases with increasing energy at 944 cm^{-1}, the population distribution is also narrower than a thermal distribution even if a bottleneck is included in the model calculation.

Our calculation also answers the question of how the laser intensity affects the distribution of excess energies with which SF_6 dissociates. At energy fluences greater than about 10 J/cm^2 the average level from which dissociation occurs is determined by the intensity for pulse durations longer than 0.6 ns. We call this regime lifetime limited because dissocation occurs primarily from levels where the RRKM predicted dissociation rate is approximately equal to the up-excitation rate. At energy fluences below about 5 J/cm^2 the calculation predicts that most of the dissociation occurs after the laser pulse is over. Then, it is the energy fluence and not the intensity which determines the average dissociation level. Figure 15 illustrates both of these considerations by showing the distribution of excess energies from which SF_6 dissociates into SF_5 + F using a 7.5 J/cm^2 laser pulse at two different pulse durations - 60ns and 0.6ns FWHM. Because the up-excitation rate is much faster with a short, high intensity laser pulse, the average excess energy is higher. However, a considerable fraction of the molecules do not dissociate during the laser pulse and are subject only to the limitation of energy fluence so that there is a long tail of population which dissociates with low excess energy. Thus, as the laser pulse duration is decreased at constant energy fluence, the molecules at first dissociate from higher energy corresponding to shorter lifetimes. In this lifetime limited region, up-excitation is balanced by dissociation. However, as the pulse duration is decreased further and in the limit of zero pulse duration, the molecules can be pumped to energy levels no higher than the levels allowed by energy fluence considerations.

Figure 16 shows the SF_5 population distribution from the model calculation for a 7.5 J/cm^2 laser pulse for the same two pulse durations - 60ns and 0.6ns FWHM. The figure shows that the average energy in SF_5 is nearly independent of the laser pulse duration. This is caused by the SF_5 quasi-continuum cross section and the SF_6 cross section above the dissociation energy being roughly the same in our model calculation. As discussed earlier, these cross sections, determined from theoretical fits of the experimental results, are about 1-2 x 10^{-19} cm^2 for SF_6 above the dissociation energy and 10^{-19} cm^2 for SF_5 in the quasi-continuum. Thus the net rate of excitation for SF_5 in the quasi-continuum and SF_6 excited above its dissociation energy are nearly the same. Most of the excess energy pumped into SF_6 appears as internal energy of SF_5. Therefore, the average energy in SF_5 does not depend very much on the amount of excess energy SF_6 has when it dissociates. Hence, it does not depend on the laser pulse duration. The shape of the SF_5 distribution is determined by (1) the distribution of excess energies with which SF_6 dissociates after the laser pulse and (2) the continuous up-pumping of population in the SF_5 quasi-continuum during the laser pulse. The SF_5 population distribution at 7.5 J/cm^2 is much broader than a thermal SF_6 distribution and is dominated by the SF_6 dissociation process. Our calculation predicts that 8% of the population is still in the discrete vibrational ladder for a 7.5 J/cm^2, 60ns laser pulse, which explains the somewhat smaller SF_5 population for the 60ns pulse than the 0.6ns pulse.

The model can also predict the dynamics of the SF_5 dissociation to SF_4 + F. For the 60 ns, 7.5 J/cm^2 pulse, the SF_5 molecules dissociate

with an average excess energy of ~6 kcal/mole. The RRKM calculation predicts that approximately 1 kcal/mole is released into translational energy. When the energy fluence is increased to 15 J/cm^2 the SF$_5$ dissociation is then in the lifetime limited regime, the average excess energy is ~9 kcal/mole, and an average of 1.5 kcal/mole is released into translation. These results are consistent with our experimental results and confirm the validity of our model for the two step dissociation process.

DISCUSSION

Our observations on the multiphoton dissociation of SF_6, like other simple bond rupture reactions studied by this group,[19] are consistent with the RRKM statistical theory as the description of unimolecular reactions in MPD. Specifically, (1) SF_6 dissociates through the lowest energy channel, $SF_5 + F$, (2) the observed SF_5 angular and velocity distributions can be fit with distributions calculated using RRKM theory, (3) the observed limits to the lifetime are in agreement with the RRKM predicted lifetime based on the excess energy which is used to fit the angular and velocity distributions, and (4) these results are in agreement with the predictions of the model calculations.

We expect that the amount of $SF_4 + F_2$ formed by SF_6 MPD is very small. However, the limited experimental sensitivity does not allow us to detect $SF_4 + F_2$ if those dissociation products are less than 20% of the SF_6 that dissociates via the $SF_5 + F$ channel. The RRKM calculation predicts the SF_6 dissociating to $SF_4 + F_2$ is several order of magnitude smaller than the dissociation to $SF_5 + F$ for SF_6 internal energies up to 30 kcal/mole above the $SF_5 + F$ dissociation limit. The RRKM theory is thus consistent with our experimental observation of SF_5 being the major dissociation product.

The comparison between calculated and observed velocity and angular distributions was made in Figs. 3 and 5. The distributions for the 5 J/cm^2 pulse fit the RRKM predicted distributions using 8 excess photons. For a 3 J/cm^2 pulse a fit is achieved using 5 excess photons. Although the error bars are relatively large, the general shape of the RRKM distribution is confirmed. For the 2.5 J/cm^2 shuttered pulse,

the angular distribution differs somewhat from the RRKM prediction using 3 excess photons because the RRKM lifetime is long than the 10 μs required to traverse the interaction region. This causes the angular distribution to peak at smaller angles as was discussed in the results and analysis section. After accounting for the finite dissociation lifetime, this result also supports the validity of the RRKM theory.

If the dissociation lifetime is appreciably shorter than the laser pulse duration, secondary multiphoton dissociation of SF_6 to SF_4+F can occur. In our experiment with laser pulses of 60 ns FWHM secondary dissociation started to appear at energy fluences of 10 J/cm^2. Thus, just below the onset of secondary dissociation the average dissociation lifetime of SF_6 should be close to 60ns. At 5 J/cm^2, somewhat below the onset of secondary dissociation, the dissociation lifetime is 50ns (8 excess photons). This result again supports the validity of the RRKM theory.

The validity of the RRKM theory indicates that even if energy is localized in certain modes immediately after the excitation, it is certainly randomized among essentially all the vibrational modes on a timescale much shorter than the dissociation lifetime. In SF_6 MPD at an intensity of 100 MW/cm^2, the net up-excitation rate is less than 10^8 photons absorbed/sec for excitation levels above the dissociation limit. Dissociation lifetimes are therefore no faster than ~10^{-8} sec. The conclusion that energy is randomized in less than 10^{-8} sec is not surprising because many experiments, reviewed by Oref and Rabinovitch[33], show that intramolecular energy transfer rates

are greater than 10^{11} sec^{-1} for polyatomic molecules when excited beyond a dissociation energy of more than 40 kcal/mole.

Initial vibrational excitation of SF_6 prior to multiphoton excitation tends to diminish the bottleneck effect of the low-lying discrete levels and thus increases the MPD yield. In our experiments SF_6 was first excited either by thermal excitation or by laser excitation. The MPD yield was then measured after further laser excitation with enough fluence. From these experiments, we can conclude:

(1) Excitation over the discrete states has a spectrum fairly close to the linear absorption spectrum of the molecules if the laser intensity is not excessively high and molecules are not internally excited. Both the 210 K (see Fig. 6) and the two frequency (see Fig. 9) multiphoton dissociation have a frequency dependence that peaks 3-4 cm^{-1} below resonance and has a FWHM spread of ~8 cm^{-1}.

(2) The absorption spectrum shifts to lower frequency as the internal excitation increases. This is shown in the 450 K MPD yield frequency dependence which peaks well below (~15cm^{-1}) the resonance.

Assuming that the pump pulse is intense enough to excite a large fraction of molecules into the quasi-continuum we could then determine crudely the dispersion of the average absorption cross section of molecules in the quasi-continuum of MPD by observing the change in energy fluence threshold with frequency (Fig. 8). This is because the average excitation in the quasi-continuum depends only upon the product of the cross section and the energy fluence so that the energy fluence required to observe MPD mear threshold should be inversely proportional to the average absorption cross section in the quasi-continuum. From

Fig. 8 and the results of Gower and Billman,[23] we may conclude that the cross section decreases by a factor of 4 ± 2 when the laser frequency changes 935 to 953 cm^{-1}. This result is in good agreement with that of Nowak and Lyman.[25]

Both the laser intensity and energy fluence are important in determining the MPD yield. As is now well known, excitation over the discrete levels into the quasi-continuum depends on the laser intensity. If the laser intensity is sufficiently strong, then most of the population is excited into the quasi-continuum. This is particularly true when a short pulse with enough energy fluence for MPD is used as shown by Black et al.[12] Then, excitation through the quasi-continuum to the dissocation level depends solely on energy fluence. This has been clearly demonstrated in a number of experiments.[12-14] Above the dissociation level, both the laser intensity and energy fluence can be important in the excitation process. In the case of long laser pulses with enough fluence, the energy fluence is sufficient to pump the molecules to a much higher excitation level above the dissociation energy, but the pumping is limited by depletion of population through dissociation. The average level of excitation or the average excess energy with which the molecules dissociate is then determined by the balance between the up-excitation rates and the dissociation rate. In other words, it is the laser intensity that determines the level of excitation at high energy fluence. In the case of shorter laser pulses, with not much fluence, the average level of excitation is limited by the available laser energy fluence. Even if the laser intensity is large enough that the up-excitation rate is much higher than the

dissociation rate, there is not enough energy fluence in the pulse to pump the molecules to higher levels. In the intermediate cases, the physical argument here suggests that both the laser intensity and the energy fluence should be important in determining the average level of excitation of SF_6 when it dissociates (see Fig. 15).

Our model calculations show that for SF_6 subject to a laser pulse with energy fluence below 5 J/cm^2 and intensity above 30 MW/cm^2, the average level of excitation is mainly determined by the energy fluence. This agrees with our experiment as shown in Fig. 17 where we compare the dissociation yields from laser pulses with energy fluence and peak intensity of 2.5 J/cm^2, ~200 MW/cm^2; 3 J/cm^2, ~60MW/cm^2; and 5 J/cm^2, ~100 MW/cm^2. If the laser intensity determines the excess energy in these cases, we would have found that the 2.5 J/cm^2 pulse results in the highest excess energy. Instead the 2.5 J/cm^2 pulse results in the smallest amount of excess energy. The excess energy predicted by the model calculation shown in Fig. 17 is in agreement with the experiment and shows that the excess energy should not depend appreciably upon the laser intensity until the energy fluence exceeds 5 J/cm^2.

These results contrast with the experiments presented in Ref. 19 where MPD was observed at energy fluences well above the threshold for dissociation. As expected, in those cases dissociation occurs at an excitation level where the up-excitation rate equals the dissociation rate determined by the laser intensity. In SF_6, this happens with our laser pulses with energy fluences > 10 J/cm^2 at 944 cm^{-1}. When the excitation level is limited by the laser intensity (and the

dissociation rate), significant dissociation will occur during the laser pulse. Then, the dissociation product can absorb more photons from the laser pulse and undergo a secondary dissociation. Thus, at higher laser fluences, the onset of secondary dissociation in SF_6 is closely associated with intensity-limited excitation. The conclusions for SF_6 should apply in general to MPD of other large polyatomic molecules.

CONCLUSION

In our experiments, the collisionless environment of the molecular beam enabled us to study many aspects of MPD of single, isolated molecules. In particular, we have investigated the effects of (1) initial vibrational excitation, (2) laser pulse duration, (3) laser energy fluence, and (4) laser frequency on the MPD of SF_6. These experiments provide quantitative results for the following processes in MPD: (1) intensity-dependent excitation over the discrete levels, (2) energy fluence dependent excitation in the quasi-continuum, and (3) excitation above the dissociation level including the subsequent dissociation dynamics.

The excitation over the discrete levels tends to limit the fraction of SF_6 molecules that can dissociate. This happens if the molecules have little initial vibrational excitation, if the laser pulse has a low intensity, or if the laser frequency is far off the peak of the linear absorption spectrum.

In the quasi-continuum more photons are absorbed by stepwise resonant excitations. Here, the excitation rate should be proportional to the laser intensity, but the average level of excitation for molecules in the quasi-continuum and the shape of the population distribution should depend only on the energy fluence. The absorption spectrum in the quasi-continuum broadens and shifts to lower energy as the excitation increases. In this way, the absorption cross section depends on the laser frequency in the quasi-continuum, and hence on the excitation rate.

The observed dissociation rates and the overall dissociation dynamics are in good agreement with predictions from the RRKM theory.

The RRKM theory assumes that the excitation energy in a molecule randomly distributes in all vibrational modes in times much shorter than the dissociation lifetime. This assumption results in a dissociation rate constant that increases rapidly with increasing energy. At sufficiently high energy fluence, when molecules dissociate mostly during the laser pulse, the level from which molecules dissociate is limited by the laser intensity such that the up-excitation rate equals the dissociation rate. If the molecules dissociate after the laser pulse is over, it is because they are in excitation levels with long dissociation lifetimes, so that the excitation level is not determined by the competition of up-excitation and dissociation, but rather by the laser energy fluence. Thus, dissociation of molecules near the energy fluence threshold for observation of MPD occurs in general after the laser pulse is over.

In many gas cell experiments on SF_6 MPD, it has been assumed that the experiment is carried out under collisionless conditions if the laser pulse duration is shorter than the average collision time. Although this assumption is valid for the measurement of absorption, the dissociation yield is affected by collisions that occur after the laser pulse. SF_6 molecules that absorb one or two excess photons have a dissociation lifetime in the millisecond time regime; much longer than typical collision times in any experiment performed at low pressure. Consequently, the gas cell measurement of dissociation yields near the energy fluence threshold never occurs in a collisionless environment.

Although recently some people have expressed doubts concerning the similarities between SF_6 MPD and the MPD of other molecules, the

experiments and model calculations described here elucidate dissociation characteristics generally applicable to the MPD of many other polyatomic molecules. Specifically, (1) at higher energy fluence the dissociation product often absorbs more energy to undergo secondary dissociation.[11,19,34] (2) Dissociation on the nanosecond timescale can be accurately modeled by the RRKM statistical theory.[19] (3) The absorption of infrared photons occurs via two steps: first an excitation over the discrete vibrational ladder and then excitation through the quasi-continuum.[1] Thus, a model calculation similar to the one we have presented here for SF_6 can also be applied to the MPD of many other polyatomic molecules. The experiments and model calculations show that though SF_6 multiphoton dissociation can be understood, experimental results are often rather complicated, depending on laser intensity, energy fluence, frequency, and molecular vibrational temperature.

ACKNOWLEDGMENTS

Appendix

Our RRKM computations have been performed using a computer program written by W. L. Hase and D. Bunker. In the initial calculations a dissociation energy of 77 kcal/mole was used; however, evidence has accumulated to show that the correct dissociation energy should be closer to 93 kcal/mole.[16] In the present calculation, we used a bond energy of 93 kcal/mole in the molecule. Fig. A1 shows the predicted RRKM rate constants for SF_6 and SF_5 as a function of excess energy.

A critical configuration is constructed by applying the minimum state density criterion. The density of states is calculated given the potential curve (assumed to be a Morse potential), vibrational frequencies and moments of inertia in the critical configuration (assumed to be functions of the reaction coordinate). The reaction coordinate is taken as the S-F internuclear bond distance. The vibrational frequencies in the critical configuration are 774, 642 (2), 948(2), and 481(7) cm^{-1} and two others which depended on the reaction coordinate. The assumed 481 cm^{-1} mode is the harmonic mean of all SF bending motions. All the other frequencies are SF stretches. One of the original 948 cm^{-1} stretch modes of the unexcited SF_6 disappears because the stretching is along the reaction coordinate. The SF bending modes are weakened in the critical configuration. An empirical formula which has been found useful in RRKM calculation for calculating frequencies of the softened bending modes in the critical configuration is:

$$\nu^+(r^+) = \nu^0 \exp (-1.9 \ r^+/r^0)$$

where $r^0 = 1.56$ Å is the equilibrium bond distance and $\nu^0 = 481$ cm^{-1}

is the equilibrium frequency. The moments of inertia in the critical configuration were calculated in a straight-forward manner. The minimum density of states search results in a value of the reaction coordinate of 3.7 Å for a given excitation energy $E^+ = 117$ kcal/mole.

A similar RRKM calculation has also been performed on the $SF_5 \rightarrow SF_4 + F$ dissociation. In this RRKM calculation many guesses must be made since there is very little data (except for energetics) on the SF_5 molecule. The moments of inertia for the ground state are determined using an SF_5 geometry identical to SF_6 with one of the fluorines missing. We estimate the vibrational frequencies of SF_5 from known vibrational frequencies for SF_5Cl, SF_6, and SF_4 to be 932(2), 772(1), 642(2), 613(1), 522(3), and 344(3) cm^{-1}.

The structure of the SF_5 molecule in the critical configuration is assumed to be similar to SF_4 molecule with a SF bond stretch serving as the reaction coordinate. The frequencies in the critical configuration are 900(2), 750(1), 560(1), 510(2), 300(3), and 63(2) cm^{-1}. The rate constants determined from such an RRKM calculation are clearly much less reliable than those determined for the $SF_6 \rightarrow SF_5 + F$ dissociation. However, we expect that the calculated lifetimes for SF_5 are correct to within an order of magnitude.

REFERENCES

1. See the reviews:

   V.S. Letokhov, and C. B. Moore, Sov. J. Quantum Electron., 6, 259; R. V. Ambartzumian and V. S. Letokhov in Chemical and Biochemical Applications of Lasers, Vol. 3, ed. C. B. Moore (Academic, New York, 1977), p. 166; N. Bloembergen and E. Yablonovitch, Physics Today, 31(5), 23 (May 1978); P. A. Schulz, Aa. S. Sudbø, D. J. Krajnovich, H. S. Kwok, Y.R. Shen and Y. T. Lee, Ann. Rev. Phys. Chem. in press (1979).

2. R.V. Ambartzumian, Yu A. Gorokhov, V. S. Letokhov, G. N. Makarov, and A. A. Puretzky, JETP Lett. 23, 22 (1976); Sov. Phys. JETP 44, 231 (1976).

3. R.V. Ambartzumian, Yu A. Gorokhov, V. S. Letokhov, G. N. Makarov, and A. A. Puretzky, JETP Lett., 23, 22 (1976); Sov. Phys. JETP 44, 231 (1976).

4. J.L. Lyman, R. J. Jensen, J. Rink, C. P. Robinson, and S. D. Rockwood, Appl. Phys. Lett., 27, 87 (1975).

5. K.C. Kompa, in Tunable Lasers and Applications, ed. A Mooradian, T. Jaeger, P. Stokseth (Springer, Berlin, 1976), p. 177.

6. M.J. Coggiola, P. A. Schulz, Y. T. Lee, and Y. R. Shen, Phys. Rev. Lett., 38, 17 (1977).

7. R.V. Ambartzumian, Yu A. Gorokhov, V. S. Letokhov, and G. N. Makarov, Sov. Phys. JETP 42, 993 (1975).

8. C.R. Quick, Jr. and C. Wittig, Chem. Phys. Lett., 48, 420 (1977).

9. J.M. Preses, R. E. Weston, Jr., and G. W. Flynn, Chem. Phys. Lett. 48, 425 (1977).

10. G.J. Diebold, F. Engelke, P. M. Lubman, J. C. Whitehead, and R. N. Zare, J. Chem. Phys., 67, 5407 (1977).

11. E.R. Grant, M. J. Coggiola, Y. T. Lee, P. A. Schulz, Aa. S. Sudbø, and Y. R. Shen, Chem. Phys. Lett., 52, 595 (1977).

12. J.G. Black, P. Kolodner, M. J. Shultz, E. Yablonovitch, and N. Bloembergen, Phys. Rev. A., 19, 704 (1979).

13. J.L. Lyman, and S. D. Rockwood, J. Appl. Phys. 47, 595 (1976).

14. J.G. Black, E. Yablonovitch, N. Bloembergen, and S. Mukamel, Phys. Rev. Lett., 38, 1131 (1977).

15. E.R. Grant, P. A. Schulz, Aa. S. Sudbø, Y. R. Shen, and Y. T. Lee, Phys. Rev. Lett., 40, 115 (1978).

16. J.L. Lyman, J. Chem. Phys., 67, 1868 (1977).

17. J. D. Lambert, D. G. Parks-Smith, and J. L. Stretton, Proc. Roy. Soc. A282, 380 (1964).

18. Y.T. Lee, J. D. McDonald, P. R. Le Breton, and D. R. Herschbach, Rev. Sci. Instu., 40, 1402 (1969).

19. Aa.S. Sudbø, P. A. Schulz, E. R. Grant, Y., R. Shen, and Y. T. Lee, J. Chem. Phys., 69, 2312 (1978).

20. P.J. Robinson and K. A. Holbrook, "Unimolecular Reactions" (Wiley, London, 1972); W. Forst. "Theory of Unimolecular Reactions" (Academic Press, New York, 1973).

21. M.J. Shultz, and E. Yablonovitch, J. Chem. Phys., 68, 3009 (1978).

22. H.S. Kwok and E. Yablonovitch, Phys. Rev. Lett., 411, 745 (1978).

23. M.C. Gower, and K. W. Billman, Opt. Commun., 20, 123 (1977).

24. F. Brunner, and D. Proch, J. Chem. Phys., 68, 4936 (1978).

25. A.V. Nowak, and J. L. Lyman, J. Quant. Spectrosc. Radiat. Transfer, 15, 945 (1975).

26. T. F. Bott, Appl. Phys. Lett, 32, 624 (1978).

27. Aa.S. Sudbø, P. A. Schulz, D. J. Krajnovich, Y. T. Lee, and Y. R. Shen, Opt. Lett., to be published.

28. R.V. Ambartzumian, N. P. Furzikov, Yu A. Gorokhov, V. S. Letokhov, G. N. Makarov, and A. A. Puretzky, JETP Lett., 23, 217 (1976); Opt. Commun., 18, 517 (1976).

29. W. Fuss, Chem. Phys., 36, 135 (1979).

30. D.M. Larsen, and N. Bloembergen, Opt. Commun. 17, 254 (1976).

31. H.W. Galbraith, and J. R. Ackerhalt, Opt. Lett., 3, 109 (1978); Opt. Lett., 3, 152 (1978); J. R. Ackerhalt and H. W. Galbraith, J. Chem. Phys., 69, 1200 (1978).

32. I.N. Knyazev, V. S. Letokhov, and V. V. Lobko, Opt. Commun., 25, 337 (1978).

33. I. Oref and B. S. Rabinovitch, Acc. Chem. Res., 12, 166 (1979).

34. J. D. Campbell, M. H. Yu, and C. Wittig, Appl. Phys. Lett. 32, 413 (1978); J. D. Campbell, M. H. Yu, M. Mangir, and C. Wittig, J. Chem. Phys. 68, 3854 (1978).

Table I. Population Distribution of SF_6 at Different Temperatures

	T_v	E Ground State	P_o	$P \geqslant 1$ photon	$P \geqslant 2$ photon	$P \geqslant 3$ photon
(146 cm^{-1})	210 K	200 cm^{-1}	0.63	0.05	0.00	0.00
(208 cm^{-1})	300 K	600 cm^{-1}	0.30	0.27	0.016	0.001
(264 cm^{-1})	380 K	1080 cm^{-1}	0.15	0.46	0.09	0.014
(312 cm^{-1})	450 K	1570 cm^{-1}	0.07	0.68	0.24	0.06

FIGURES

Figure 1.   Electronics schematic of the two laser experiment. Many
of the experiments were run with just one laser operating.

Figure 2.   Angular distribution of SF_3^+ and SF_2^+ signals at high
and low laser intensity. At high laser intensity a second-
ary dissociation occurs.

Figure 3.   Velocity distribution of SF_3^+ compared with three RRKM
predicted velocity distributions. The vertical axis plots
the number density of fragments normalized to the observed
angular distribution.

        — — — — 5 excess photons

        —— - —— 8 excess protons

        ————— 12 excess protons

Figure 4.   Predicted translational energy distribution for the RRKM
calculation of the SF_6 dissociation using 2, 3, 5, 8, and
12 excess photons.

        —— - - —— 2 excess photons

        ● ● ● ● ● ● ● 3 excess photons

        — — — — 5 excess photons

        —— - —— 8 excess photons

        _____ 12 excess photons.

Figure 5. Angular distribtuion of SF_3^+ using:

$\triangle$ 5 J/cm^2 , 60ns pulse

o 3 J/cm^2 , 60 ns pulse

$\blacktriangle$ 2.5 J/cm^2, 15 ns pulse.

The angular distributions are compared with the RRKM predicted angular distributions for 2, 3, 5, 8, and 12 excess photons. Symbols as in Fig. 4.

Figure 6. Frequency dependence of SF_6 MPD at vibrational temperatures:

—— - ——   210K

——————   300K

—— —— ——   380K

● ● ● ● ● ● ● 450K

Figure 7. Energy fluence dependence of SF_6 MPD at three CO_2 laser frequencies.

Figure 8. Minimum energy fluence at which detectable SF_3^+ signal could be observed as a function of frequency.

Figure 9. Frequency spectrum of SF_6 absorption with a weak CO_2 laser pulse. Detection was achieved by dissociation with a 10 J/cm^2 laser pulse at $1060 cm^{-1}$.

● ● ● ● ● ● ● 5 J/cm^2 pulse - single frequency only

——————   1.2 J/cm^2 pulse

—— —— ——   .5 J/cm^2 pulse

The relative size of the signal for the 1.2 and .5 J/cm^2 pulses is shown in the figure. Otherwise the scale is arbitrary.

Figure 10. Model used for excitation over the discrete states. The fraction of molecules excited to the quasi-continuum is assumed to be a function of intensity only. See text for functional form.

Figure 11. Typical laser pulse shape used in the model calculations in the text. The energy fluence is 10 J/cm^2, 40% of which is in the tail.

Figure 12. Energy deposition in SF_6. $<n>$ vs. energy fluence predicted by the model calculation for two different pulse lengths 60ns and 0.6ns. These are compared with the experimental data of Black, et al.

This model calculation	Experiment of Reference 7
0.6ns pulse	————
60ns multimode	— — —
0.6ns single mode	● ● ● ●

Figure 13. SF_6 yield into SF_5 and SF_4 as a function of energy fluence predicted by the model calculation. Only those molecules which can be detected in our molecular beam experiment (lifetime less than 10μs) are considered.

Figure 14. Calculation of multiphoton excited SF_6 distribution predicted by model calculation using 0.3 J/cm^2 laser pulse.

————— 15ns FWHM - shuttered pulse

—— —— 60 ns FWHM pulse

Figure 15. Model calculation of the distribution of excess energies with which SF_6 dissociates for a 7.5 J/cm^2 pulse at pulse durations of 60 ns and 0.6 ns.

Figure 16. SF_5 population distributions immediately after irradiation

of SF_6 with 7.5 J/cm^2 pulse of different durations. The

dissociation energy of 51 kcal/mole is marked by the arrow.

_____ 0.6ns FWHM pulse

____ ____ 60ns FWHM pulse

The dotted curves indicate the distributions long after the

end of each laser pulse. After the end of the laser pulse,

all SF_6 excited beyond the dissociation limit dissociates to

SF_5, thus accounting for the increase in population of SF_5

shown by the dotted curves.

Figure 17.   Average number of excess photons absorbed by SF_6 beyond

the dissociation threshold versus energy fluence. The

experimental points are based on the agreement of the

RRKM predicted angular distribution with the experimental

angular distribution in Fig. 5. The laser pulses used

were a 2.5 J/cm^2, laser shuttered pulse and 3 and 5 J/cm^2

normal pulses. The curves show the prediction of the model

calculation ignoring half of the population with 3 excess

photons and all population which dissociate with less

than 3 excess photons because the dissociation lifetime

is longer than 10 μs.

_____ normal pulse

____ ____ shuttered laser pulse

Figure A1.   RRKM calculated rate constant using a dissociation energy

of 93 kcal/mole for $SF_6 \rightarrow SF_5 + F$ and a dissociation

energy of 51/kcal/mole for $SF_5 \rightarrow SF_4 + F$.
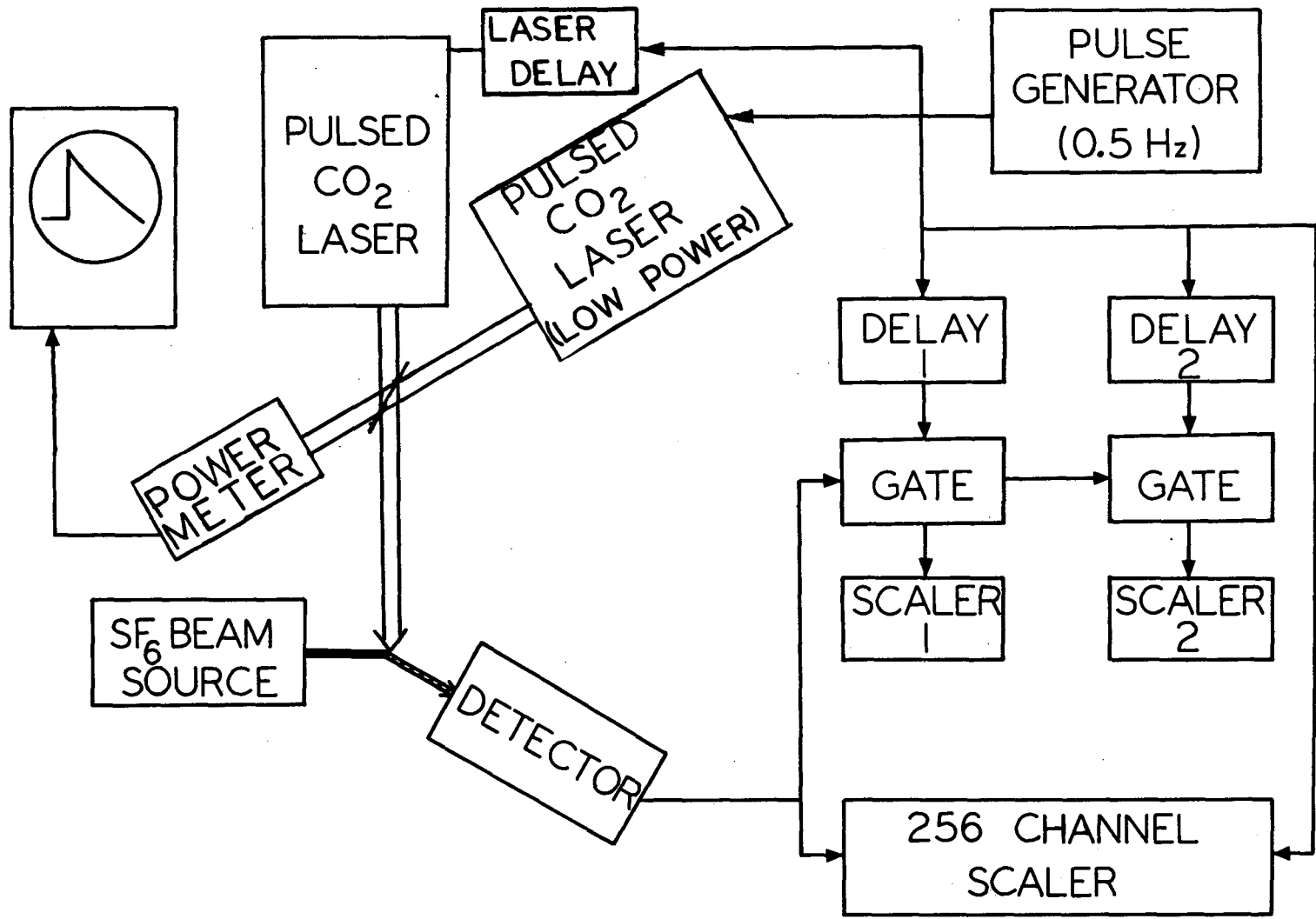
Fig. 1

-49-

Fig. 2

XBL 798-2389

$SF_6 \rightarrow \underline{SF_5} + F$

Fig. 3

XBL 792-8359

Fig. 4

XBL 792-8354

$SF_6 \longrightarrow SF_5 + F$
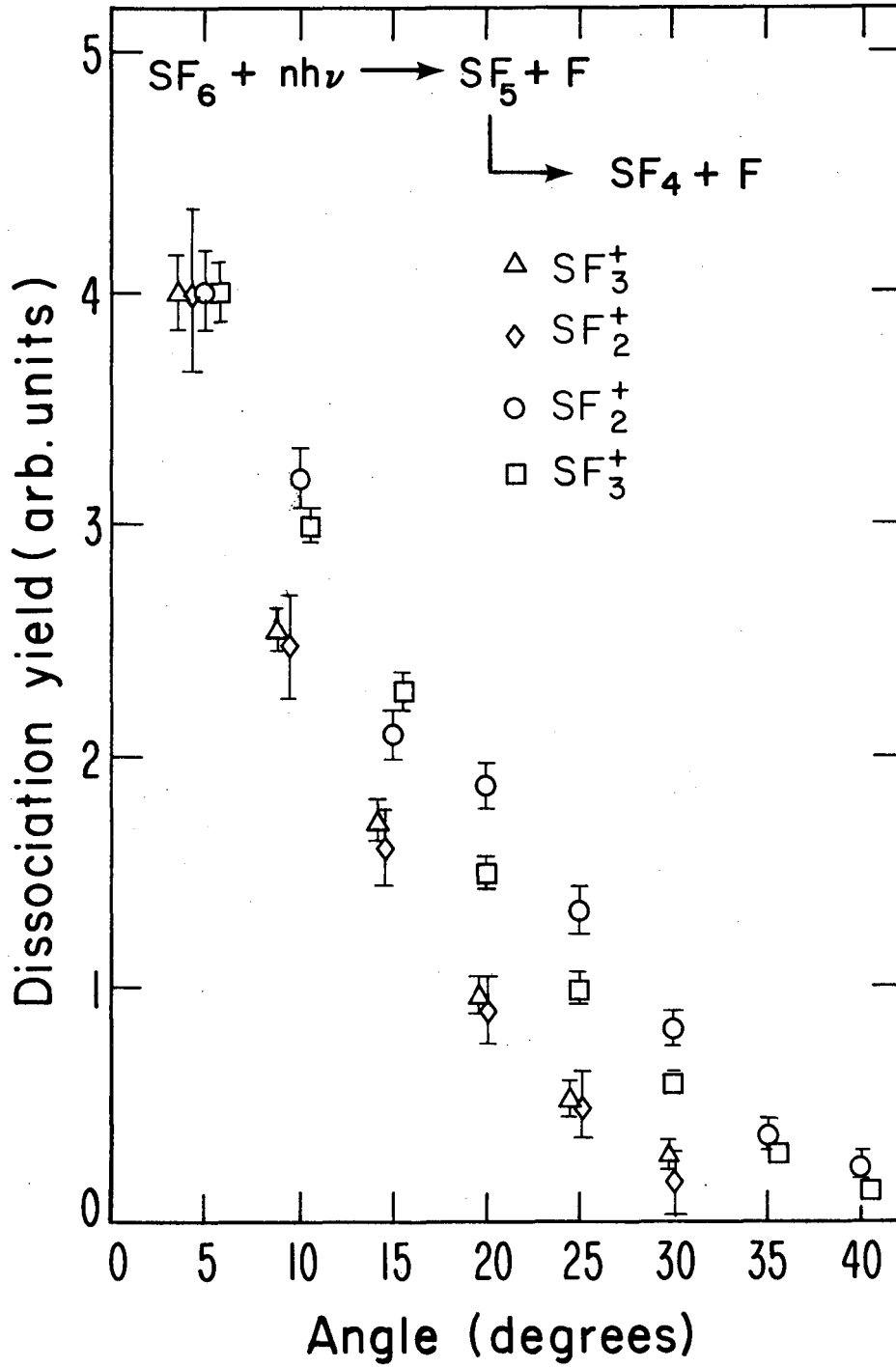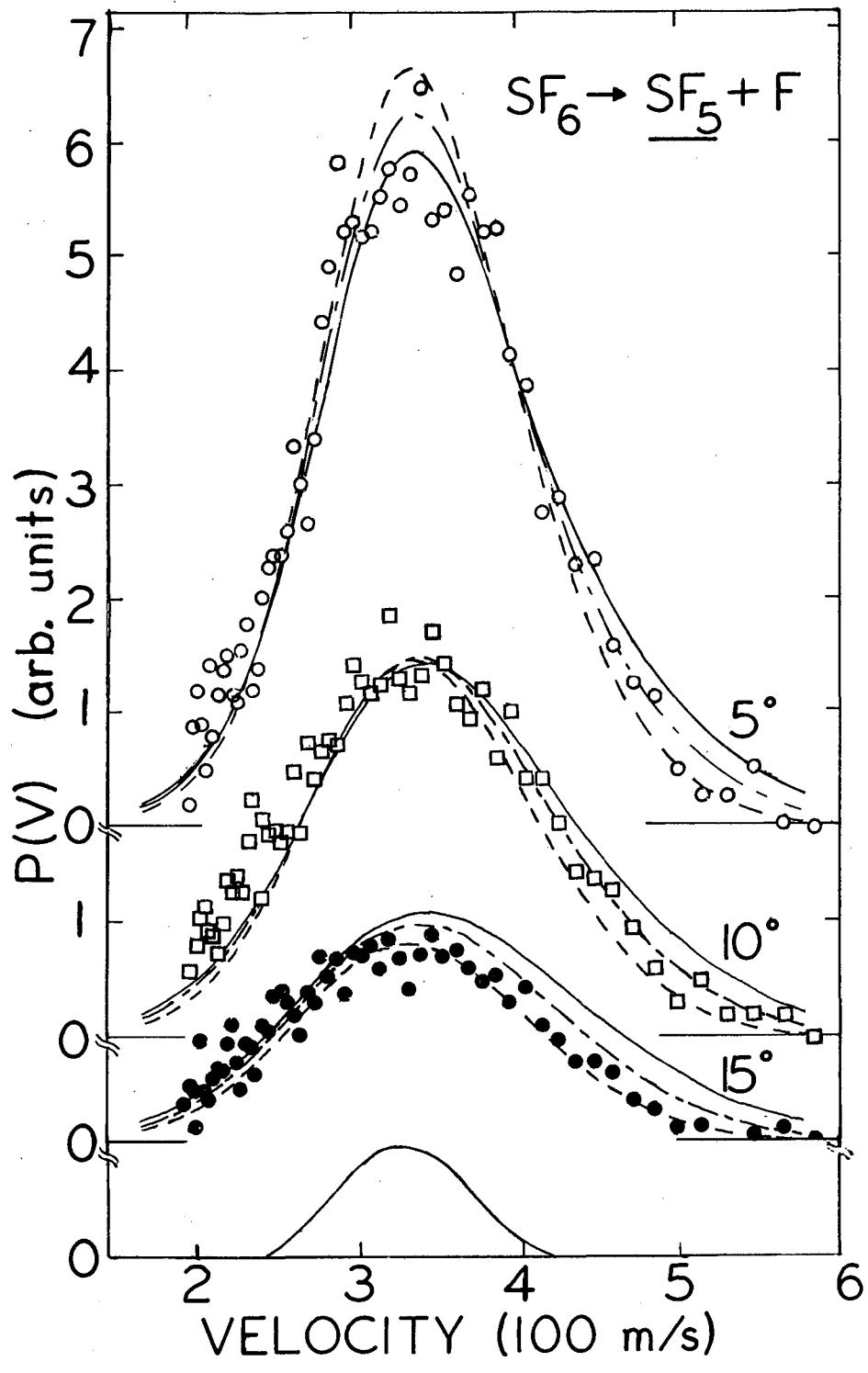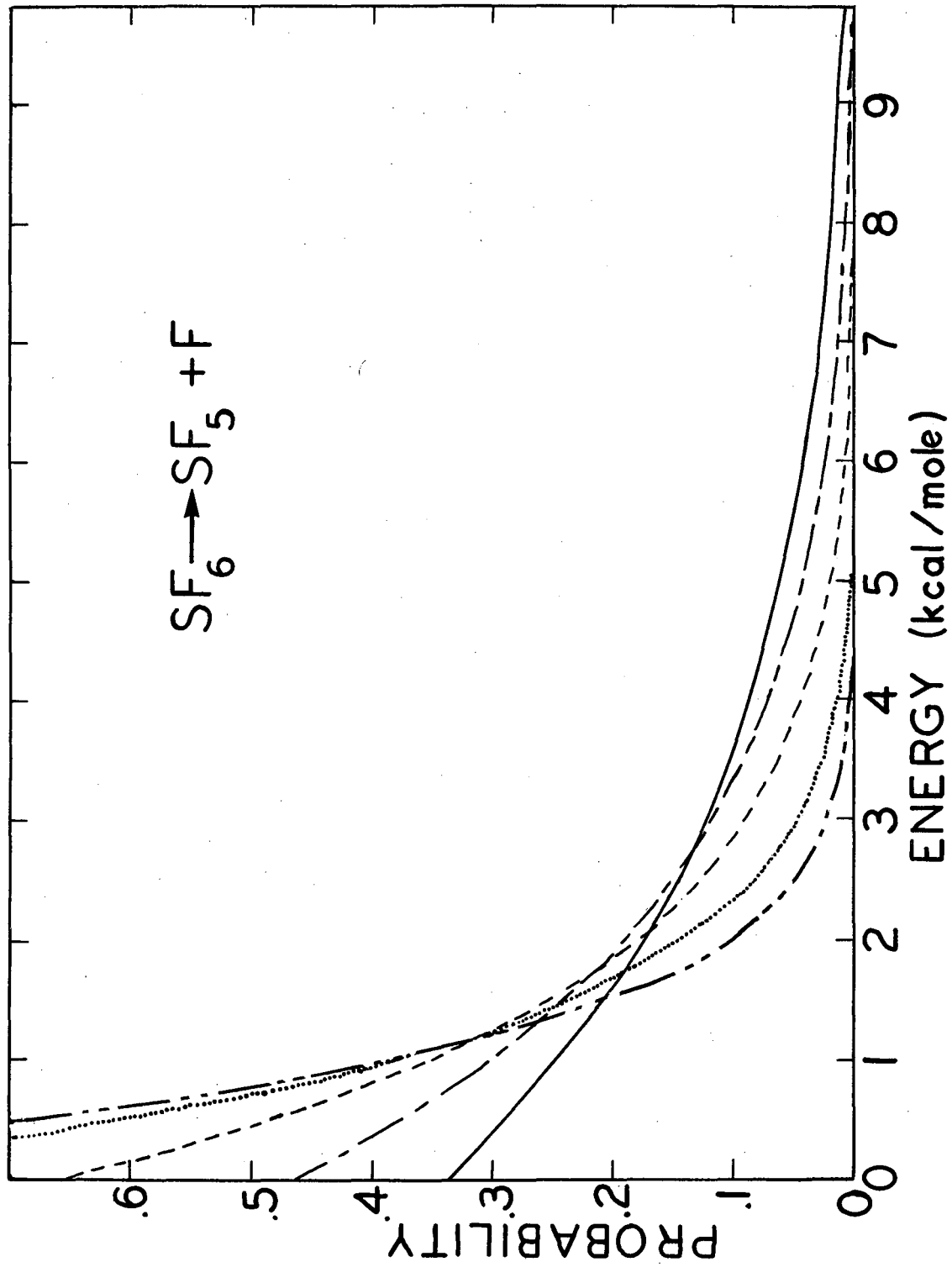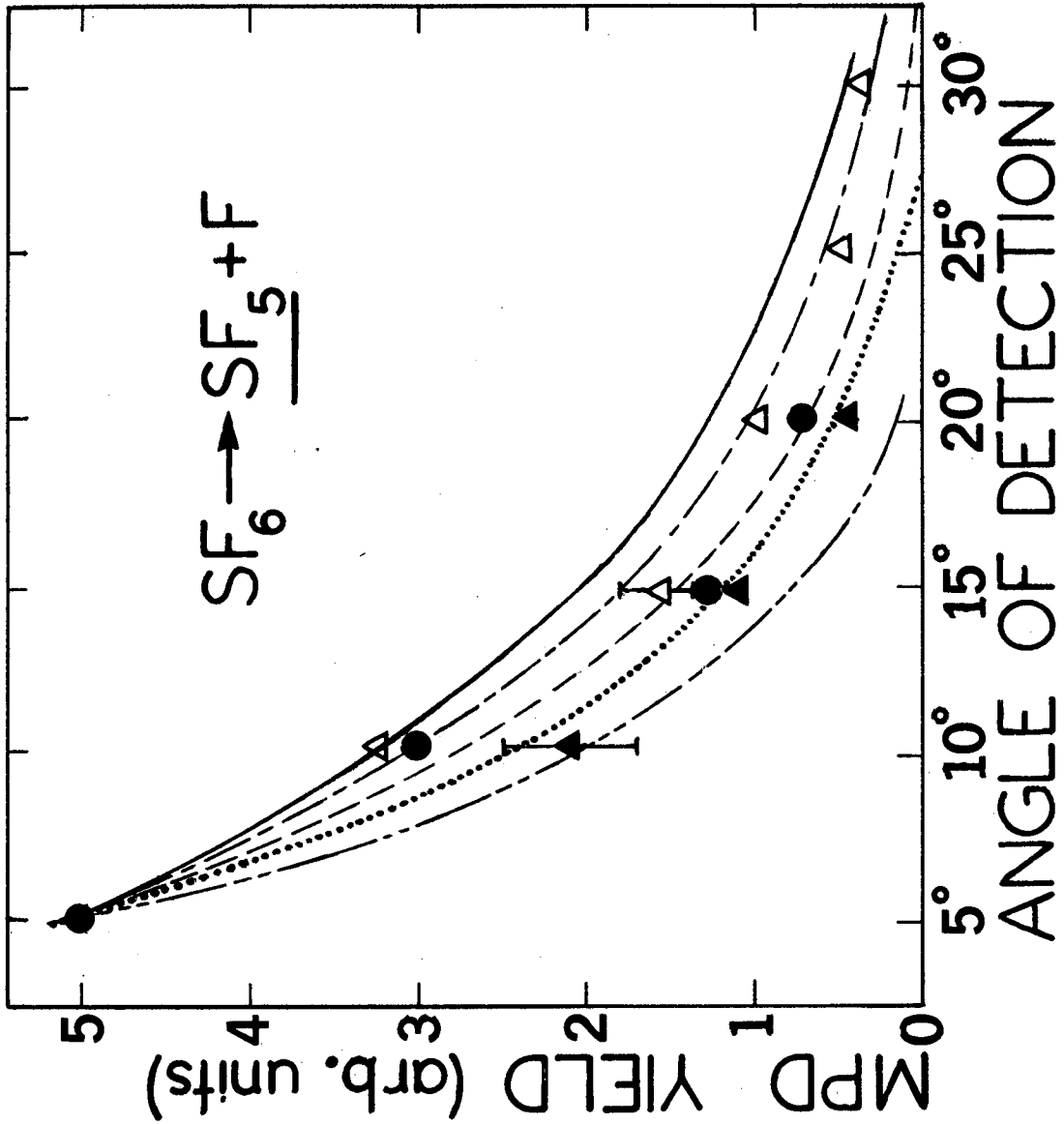
Fig. 5

XBL 785-8834
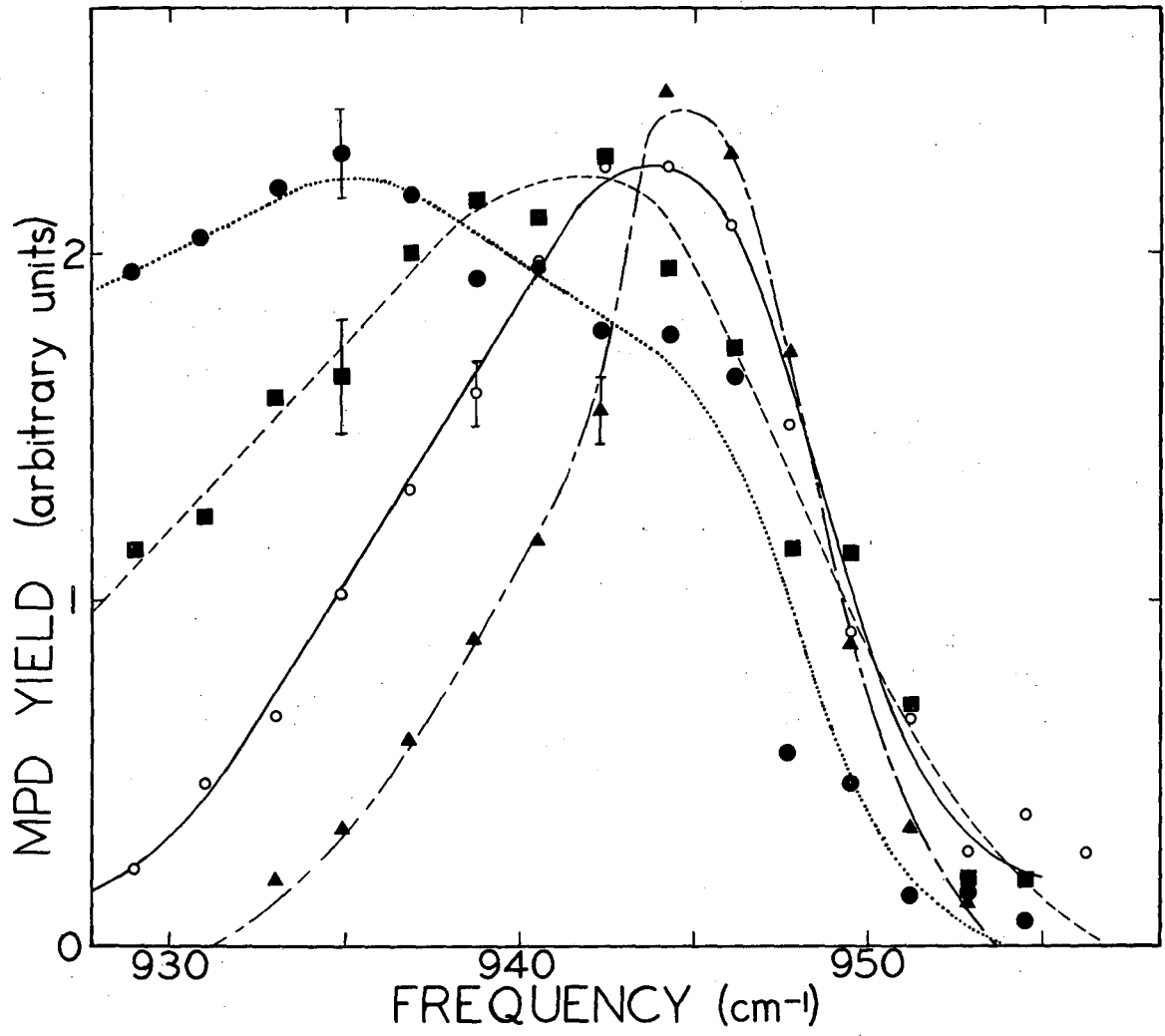
XBL 7811-13182

Fig. 6

Fig. 7

XBL 792-8358

FREQUENCY (cm⁻¹)

ENERGY INTERCEPT (J/cm²)
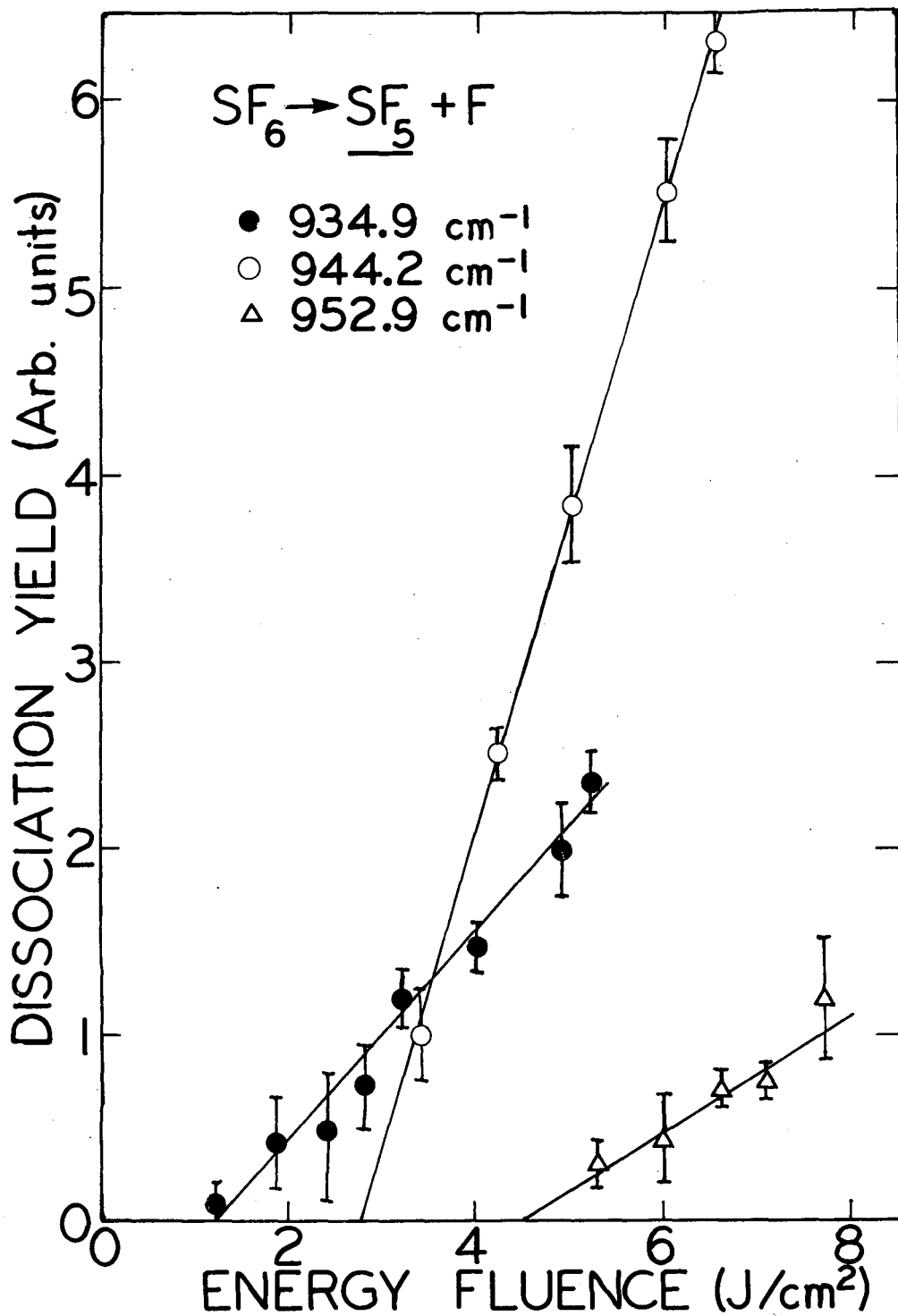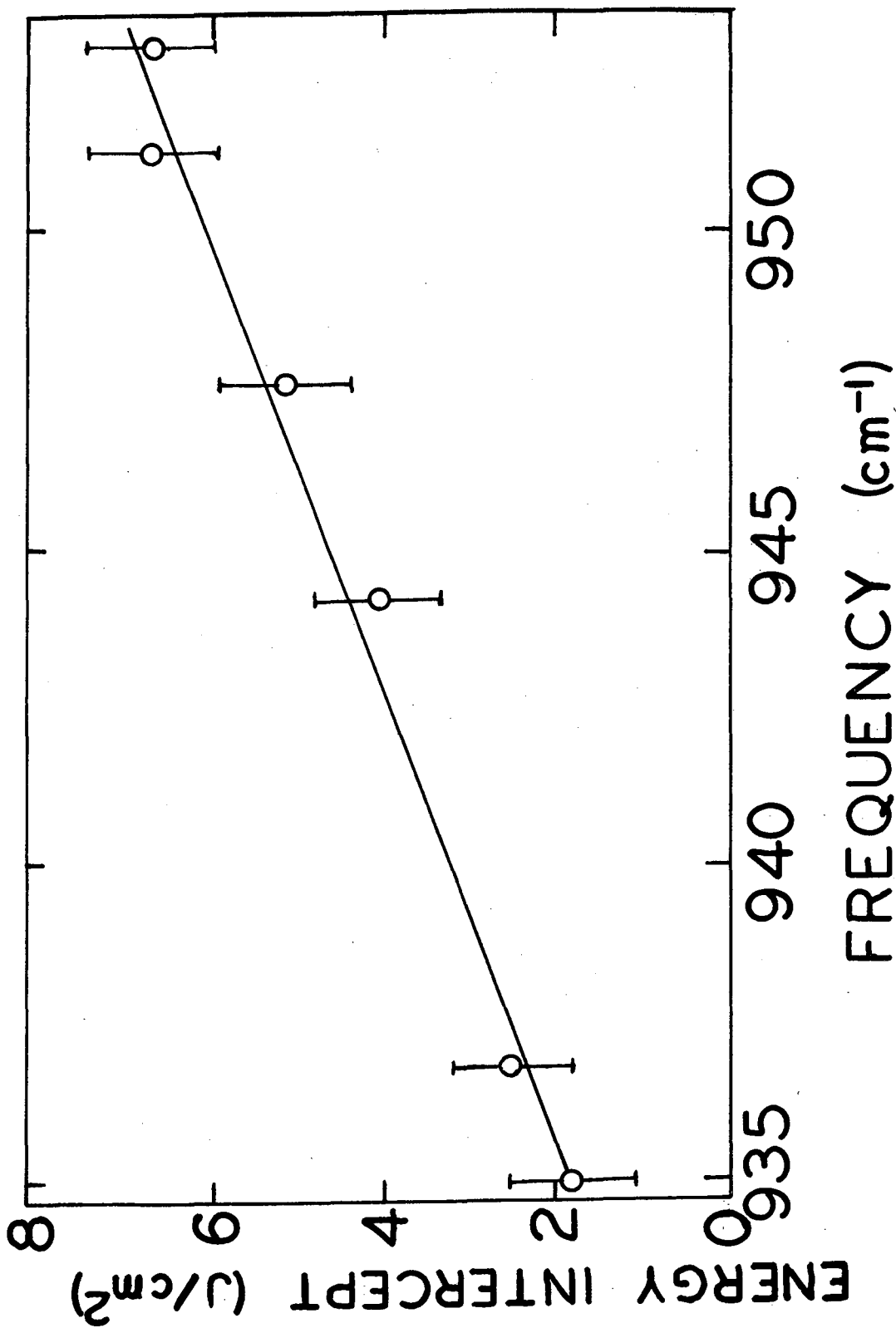
XBL 792-8282

Fig. 2
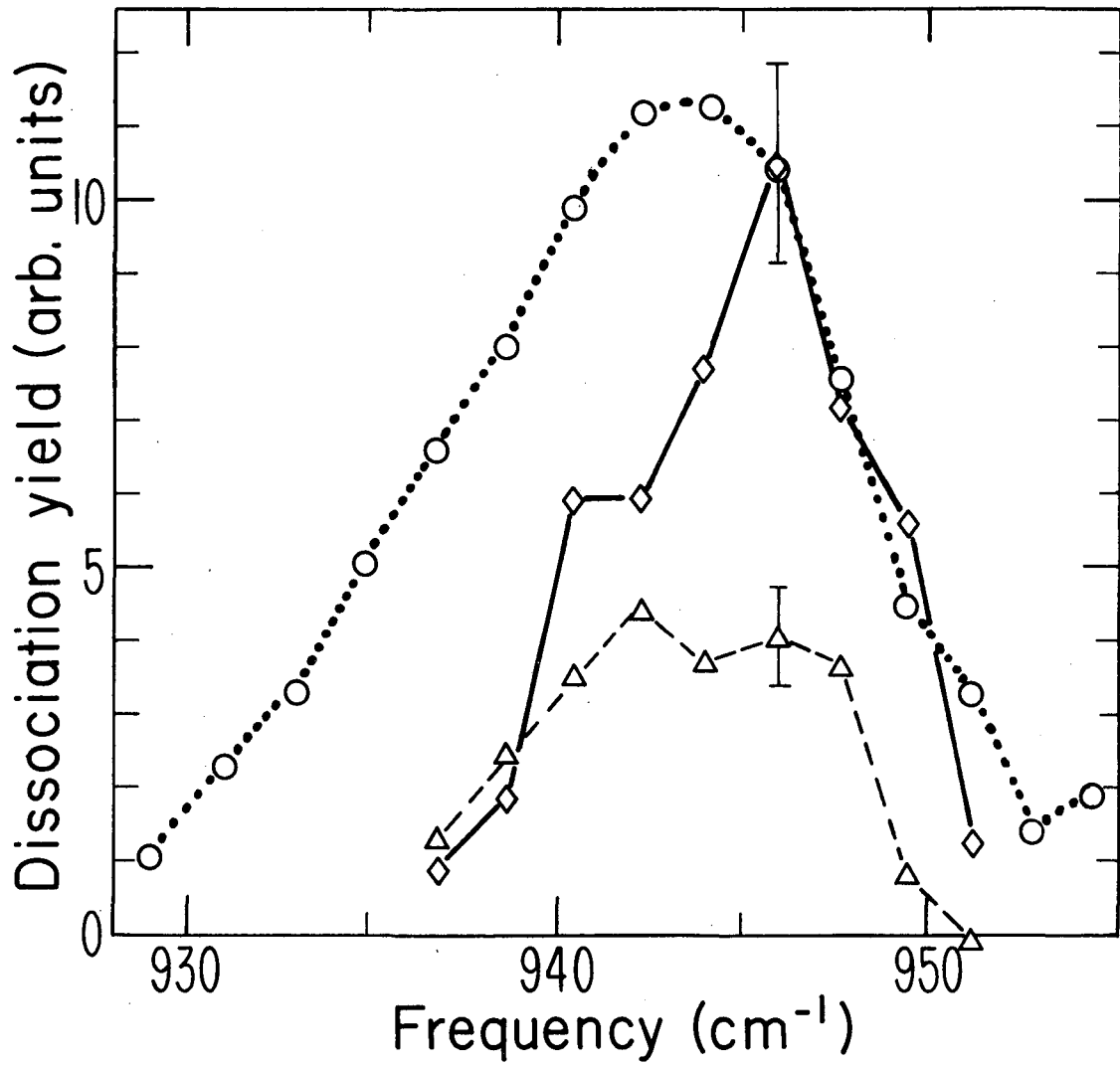
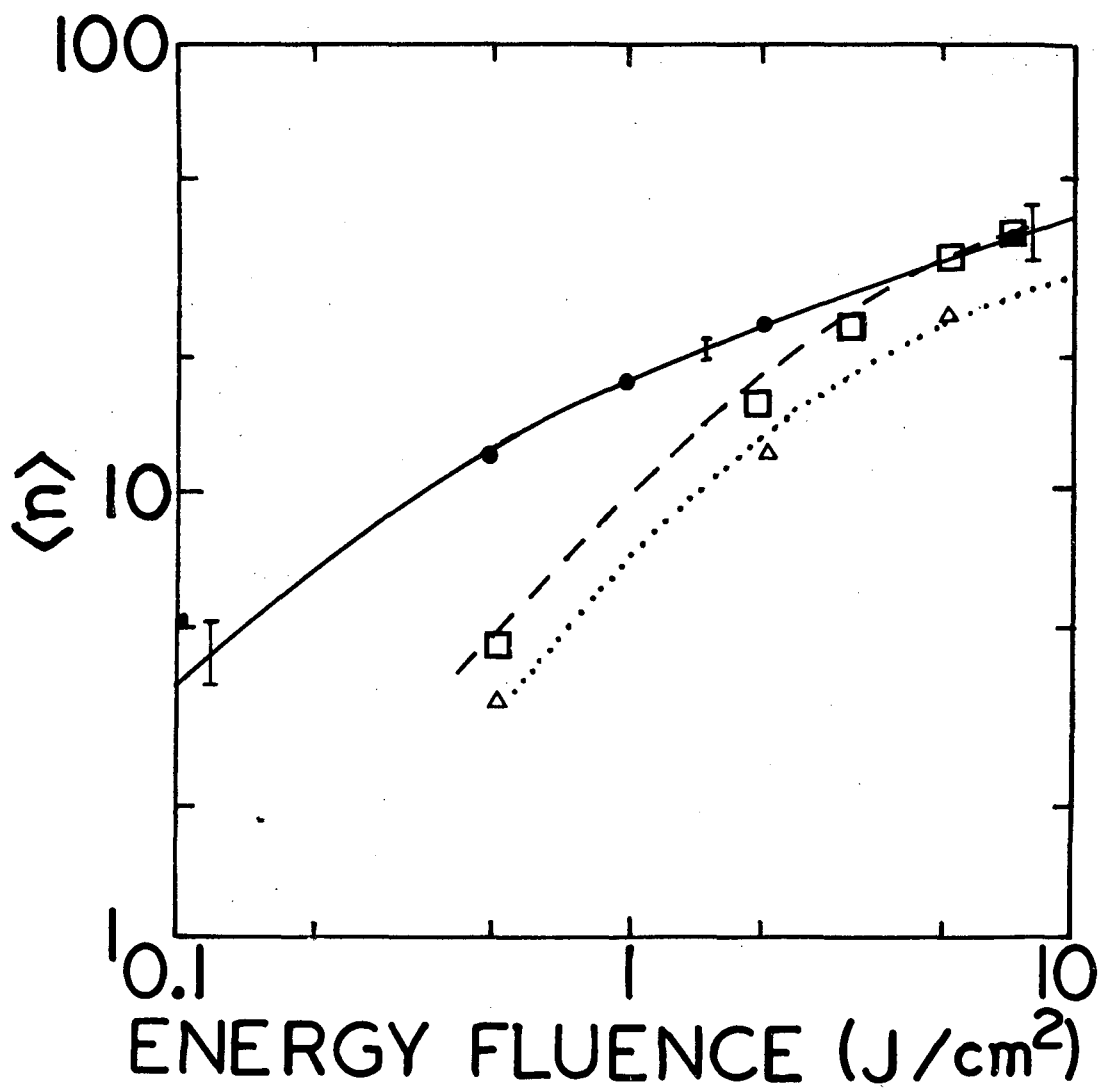XBL 798-2388

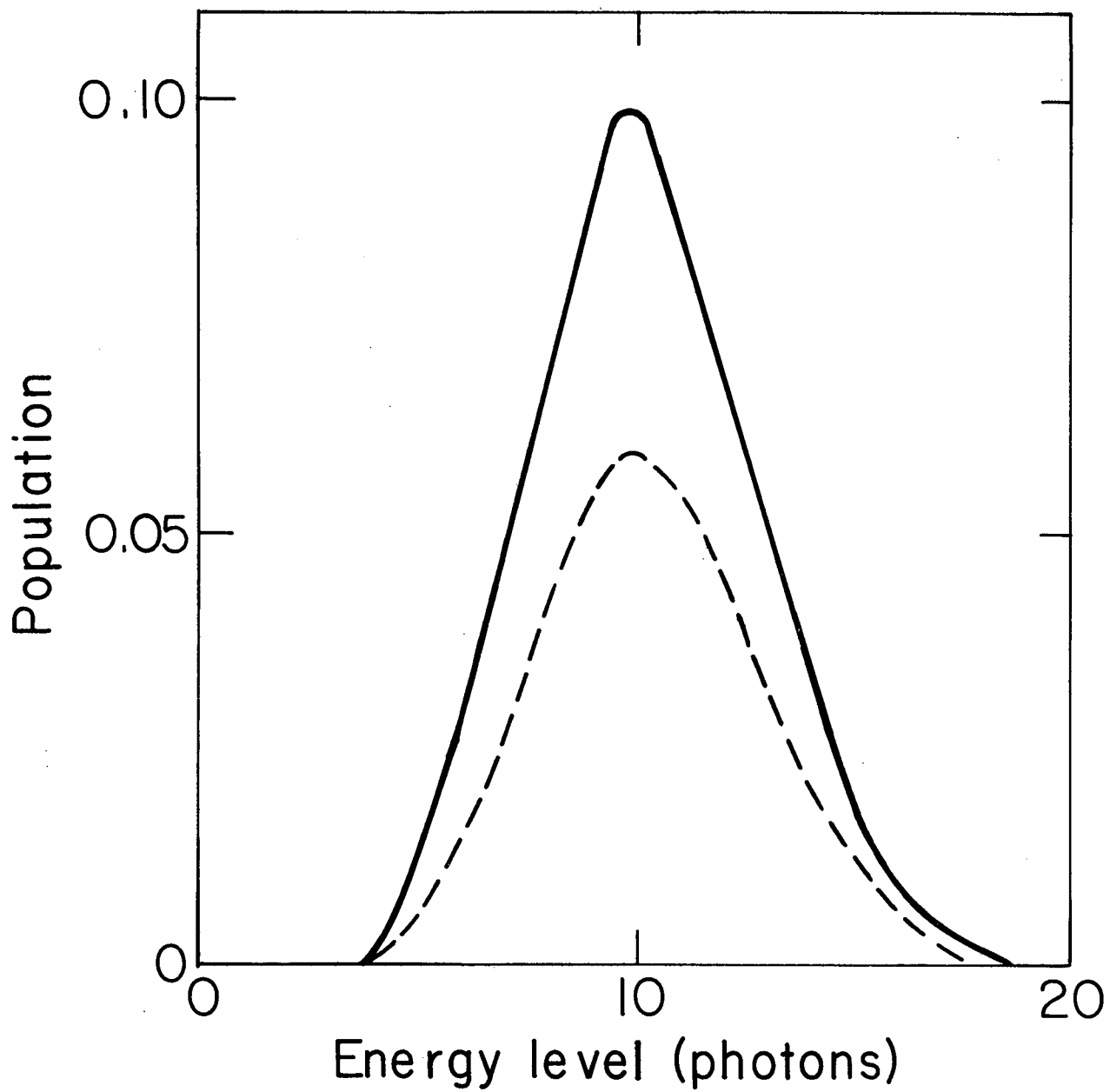Fig. 9
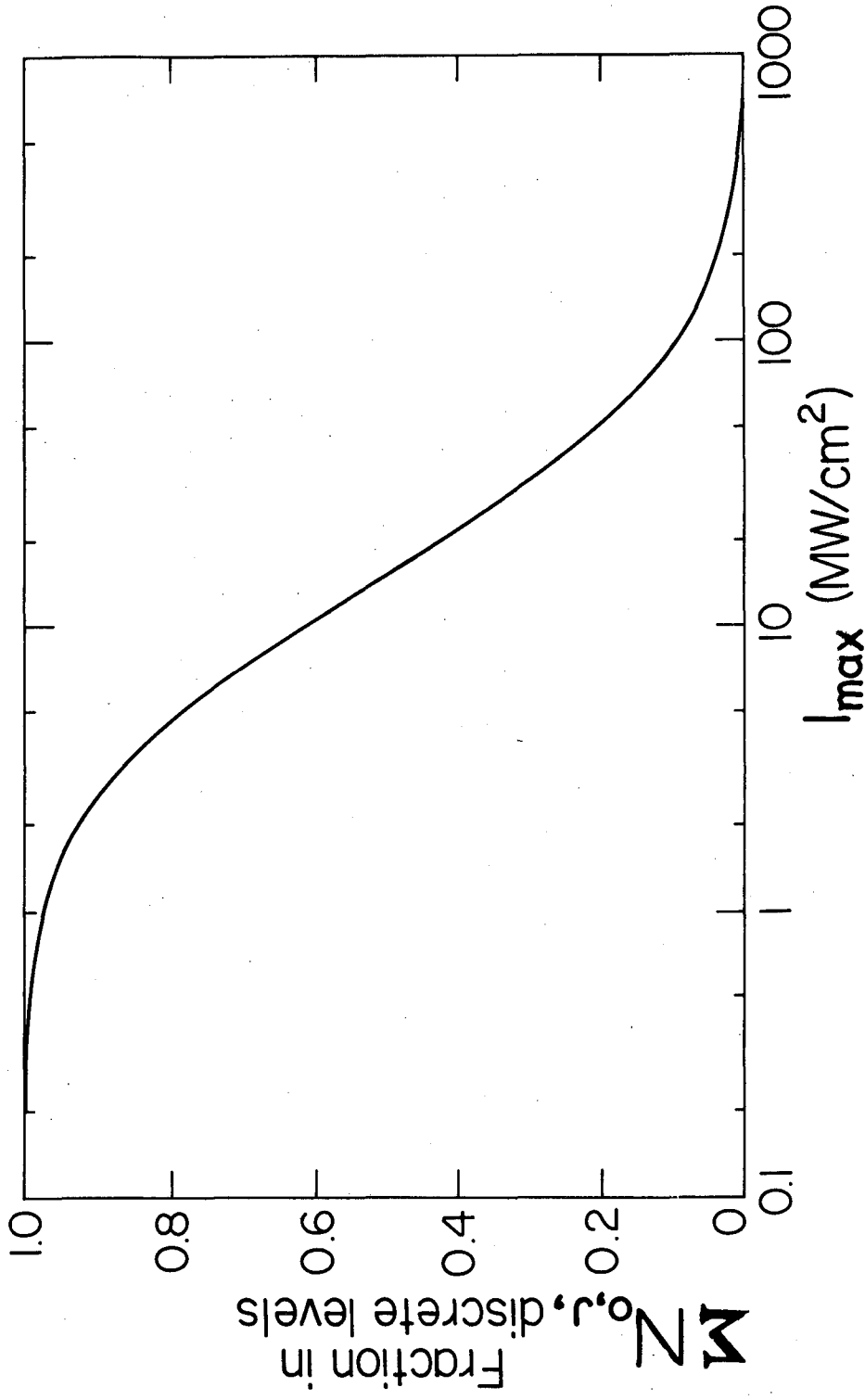
Fig. 10

XBL 795-1654A
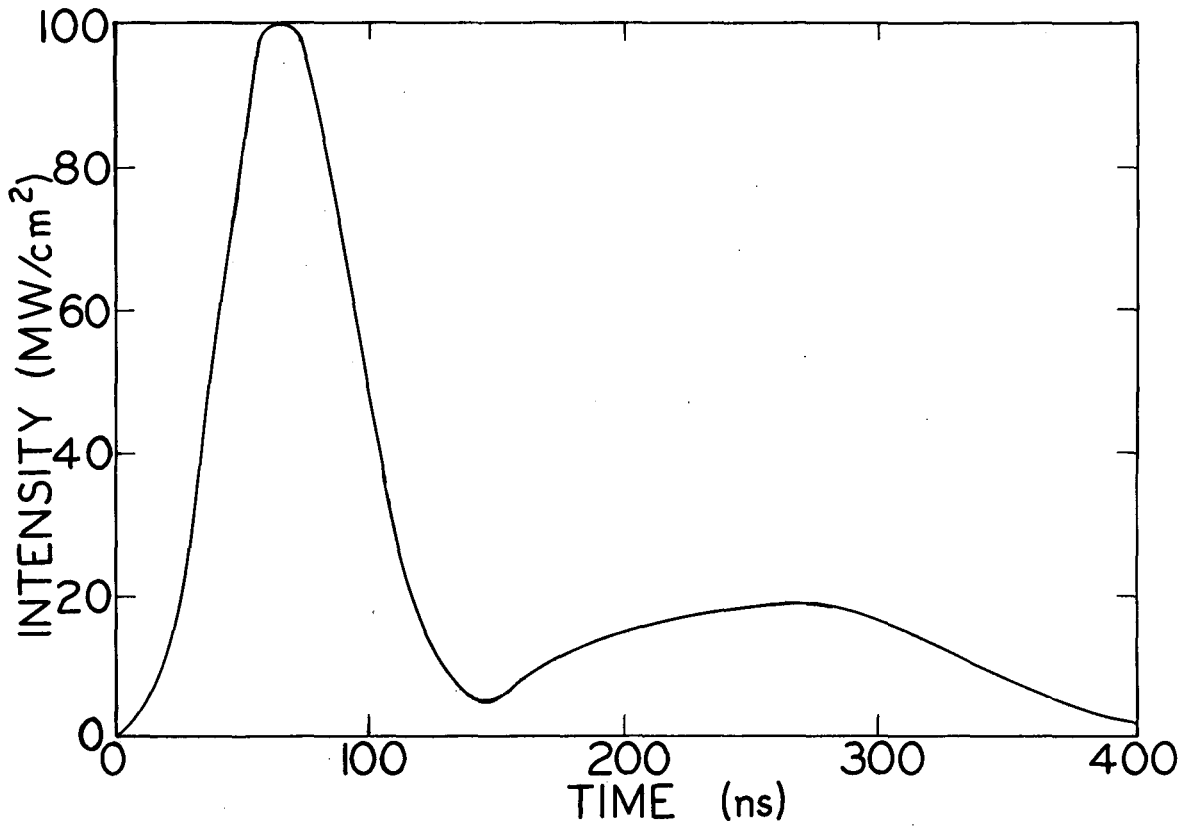
XBL 792-8356

Fig. 11

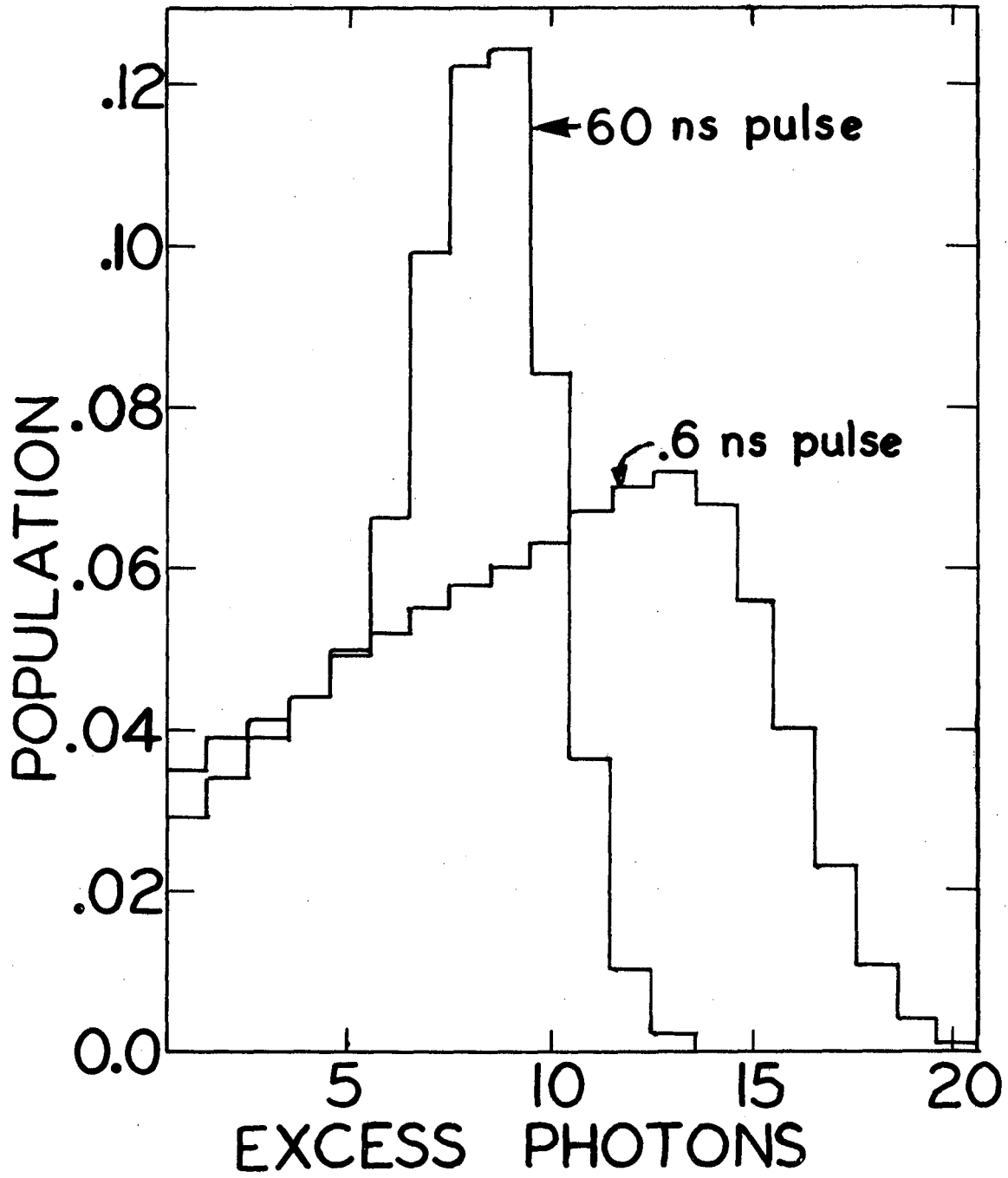Fig. 12

XBL 792-8281

XBL 798-2387
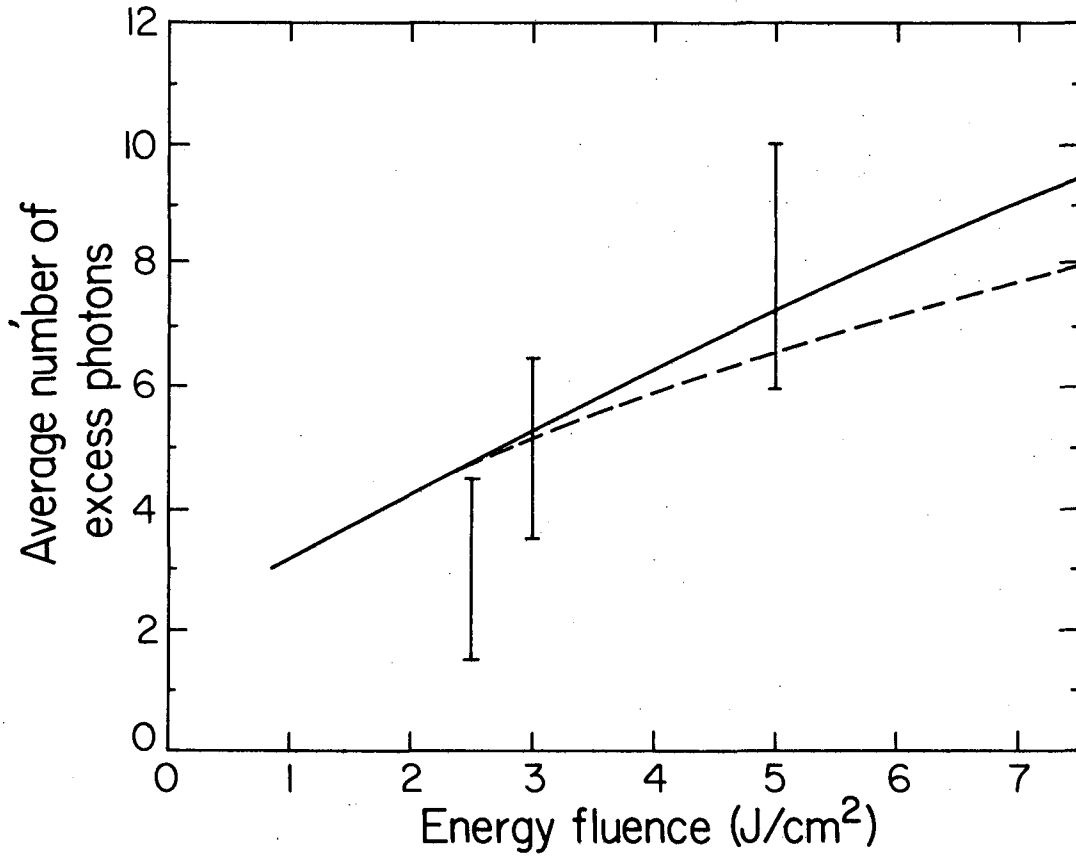
Fig. 13
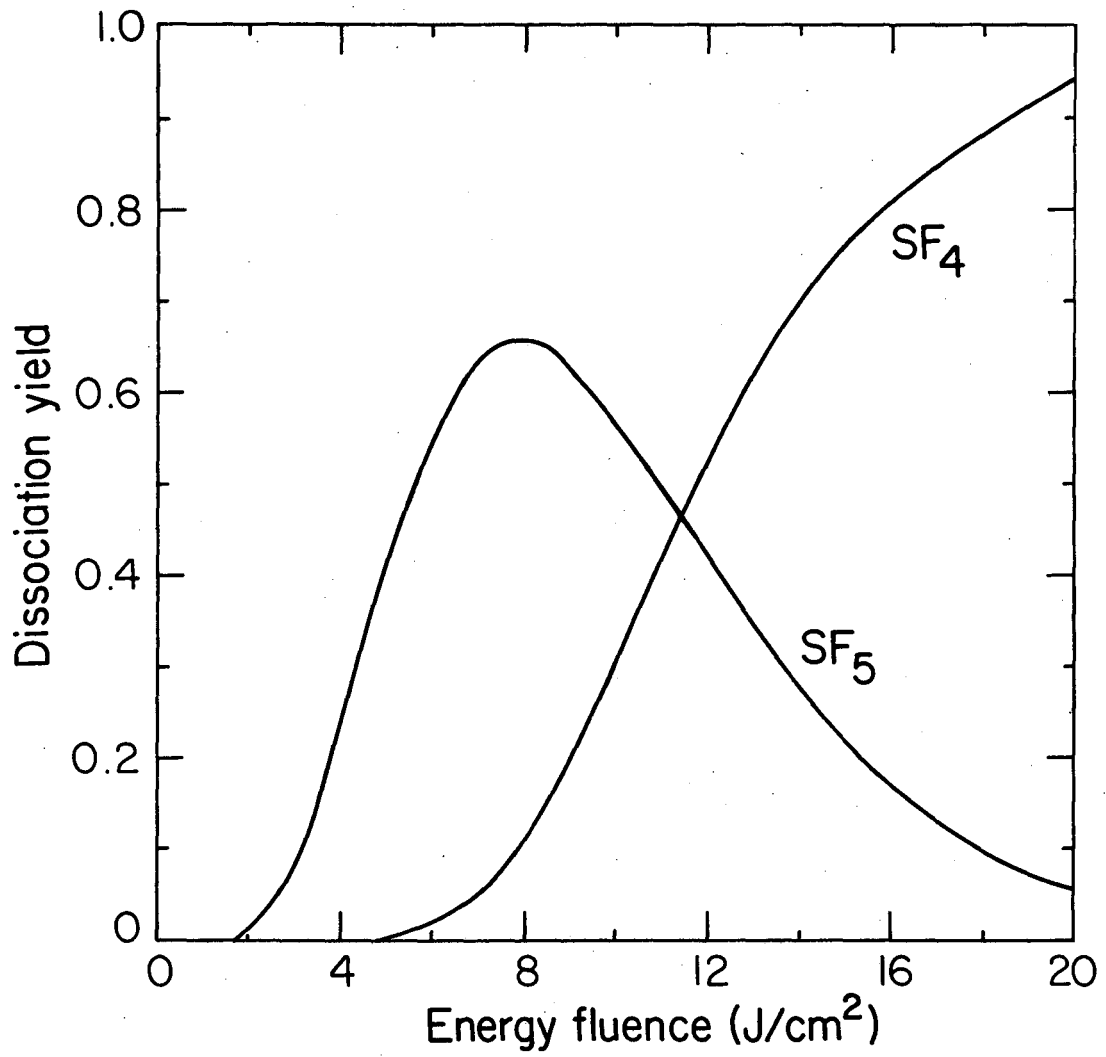
Fig. 14

XBL 795-1653

Fig. 15

XBL 798-11021
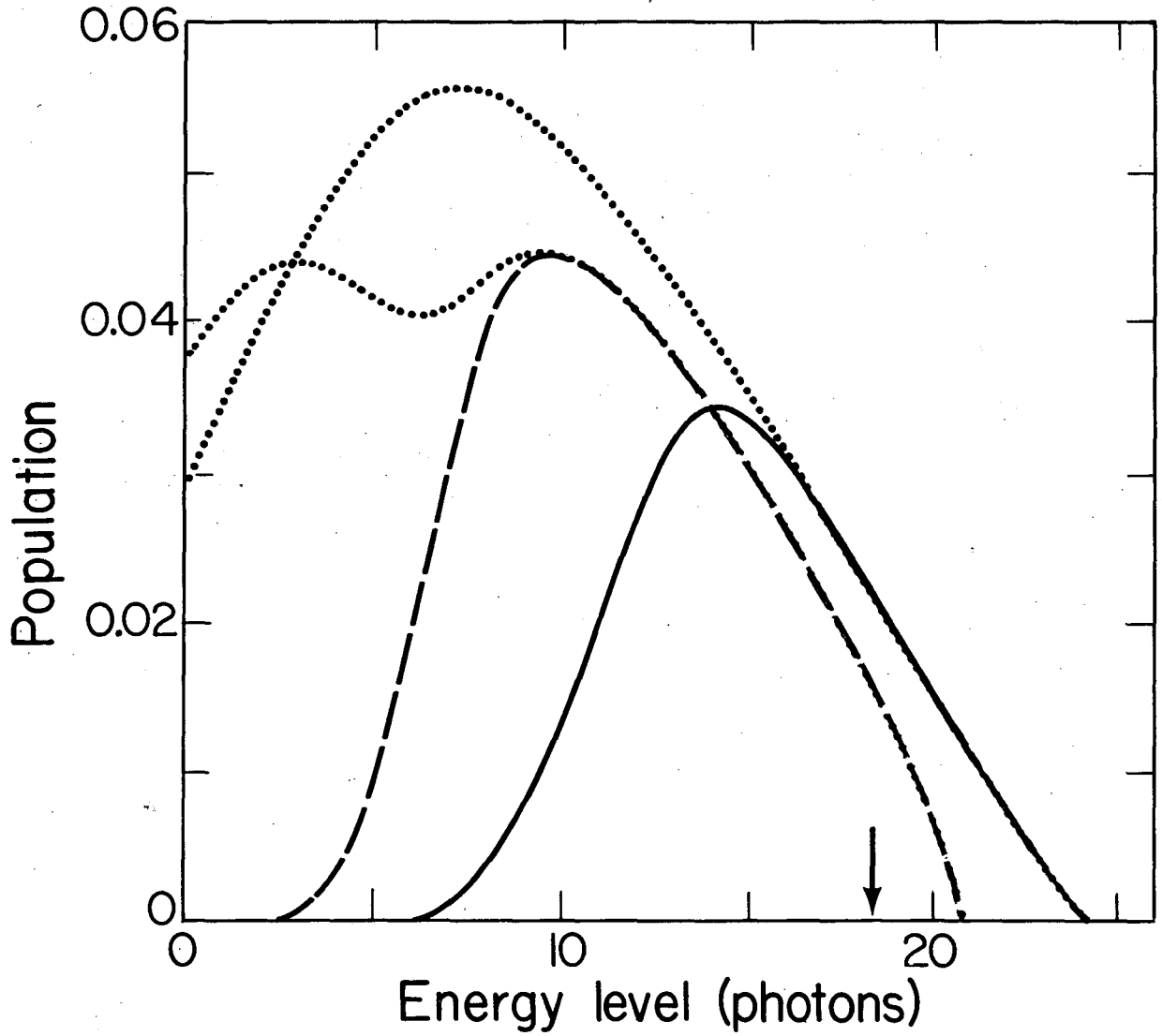
Fig. 16

XBL 798-2390

XBL 795-1652

Fig. 17

Fig. A1

XBL 792-8353